

More loops and legs in Higgs-regulated $\mathcal{N} = 4$ SYM amplitudes

Johannes M. Henn,^a Stephen G. Naculich,^{b,1} Howard J. Schnitzer^{c,2} and Marcus Spradlin^{d,3}

^a*Institut für Physik, Humboldt-Universität zu Berlin, Newtonstraße 15, D-12489 Berlin, Germany*

^b*Department of Physics, Bowdoin College, Brunswick, ME 04011, U.S.A.*

^c*Theoretical Physics Group, Martin Fisher School of Physics, Brandeis University, Waltham, MA 02454, U.S.A.*

^d*Department of Physics, Brown University, Providence, RI 02912, U.S.A.*

E-mail: henn@physik.hu-berlin.de, naculich@bowdoin.edu, schnitzr@brandeis.edu, marcus_spradlin@brown.edu

ABSTRACT: We extend the analysis of Higgs-regulated planar amplitudes of $\mathcal{N} = 4$ supersymmetric Yang-Mills theory to four loops for the four-gluon amplitude and to two loops for the five-gluon amplitude. Our calculations are consistent with a proposed all-loop ansatz for planar MHV n -gluon amplitudes that is the analog of the BDS ansatz in dimensional regularization. In all cases considered, we have verified that the IR-finite parts of the logarithm of the amplitudes have the same dependence on kinematic variables as the corresponding functions in dimensionally-regulated amplitudes (up to overall additive constants, which we determine).

We also study various Regge limits of $\mathcal{N} = 4$ SYM planar n -gluon amplitudes. Euclidean Regge limits of Higgs-regulated $n \geq 4$ amplitudes yield results similar in form to those found using dimensional regularization, but with different expressions for the gluon trajectory and Regge vertices resulting from the different regulator scheme. We also show that the Regge limit of the four-gluon amplitude is dominated at next-to-leading-log order by vertical ladder diagrams together with the class of vertical ladder diagrams with a single H-shaped insertion.

KEYWORDS: Supersymmetric gauge theory, AdS-CFT Correspondence, NLO Computations, $1/N$ Expansion

ARXIV EPRINT: [1004.5381](https://arxiv.org/abs/1004.5381)

¹Research supported in part by the NSF under grant PHY-0756518

²Research supported in part by the DOE under grant DE-FG02-92ER40706

³Research supported in part by the DOE under grant DE-FG02-91ER40688

Contents

1	Introduction	1
2	The four-point amplitude	5
2.1	Four-loop four-point amplitude	6
2.2	Regge limit of the four-point function	9
3	The five-point amplitude	12
4	Regge limits	16
4.1	The five-point amplitude	16
4.2	Regge (a) limits for $n = 5$	17
4.3	Regge (b) limits for $n = 5$	17
4.4	Regge (a) limits for $n \geq 6$	19
4.5	Regge limit (b) for $n = 6$	19
5	Summary	20
A	Regge limits of four-loop four-point integrals	21
B	Regge limit of the L-loop ladder with H-insertion	23
C	Five-point integrals	27

1 Introduction

The assumption of dual conformal symmetry has proven useful for understanding the structure of the large- N limit of higher-loop scattering amplitudes in $\mathcal{N} = 4$ supersymmetric Yang-Mills theory. Dual conformal invariance characterizes [1] the set of scalar diagrams that forms a basis for the computation of higher-loop amplitudes in the unitarity-based approach of refs. [2–6]. Moreover, coupled with the assumption of Wilson loop/MHV scattering amplitude duality [7–10], dual conformal symmetry has been used [11] to explain why maximally-helicity-violating planar n -gluon amplitudes obey the Bern-Dixon-Smirnov (BDS) ansatz [12] for $n = 4$ and 5. It also helps to explain why the BDS ansatz fails to predict the scattering amplitude starting at $n = 6$, as observed in refs. [13–16], and constrains the form of the discrepancy, called the remainder function (for reviews see refs. [17, 18]). Wilson loop/MHV amplitude duality has been used to determine the precise form of this remainder function for $n = 6$ in refs. [16, 19–21].

Scattering amplitudes in massless gauge theories possess infrared (IR) divergences that must be regulated. It is desirable that the regulator preserve as many symmetries as possible. While dimensional regularization explicitly breaks dual conformal symmetry (see, e.g.,

ref. [22]), an alternative Higgs regulator proposed by Alday, Henn, Plefka, and Schuster [23] leaves the dual conformal symmetry unbroken. In this approach, the supersymmetric Yang-Mills (SYM) theory is considered on the Coulomb branch where scalar vevs break the gauge symmetry, causing some of the gauge bosons to become massive through the Higgs mechanism. Planar gluon scattering amplitudes on this branch can be computed using scalar diagrams in which some of the internal and external states are massive, regulating the IR divergences of the scattering amplitudes. (For earlier applications of a massive IR regulator, see refs. [7, 24–27]; low-energy amplitudes in the Higgsed phase of SYM have been studied in ref. [28].) The diagrams remain dual conformal invariant, however, provided that the dual conformal generators are taken to act on the masses as well as on the kinematical variables, a generalization referred to as extended dual conformal symmetry.

The assumption of extended dual conformal symmetry¹ severely restricts the number of diagrams that can appear in the scattering amplitudes. In particular it forbids loop integrals containing triangles, which have indeed recently been shown to be absent from one-loop amplitudes on the Coulomb branch [29] (a related discussion was given in ref. [26]). At one point in moduli space, all the lines along the periphery of the diagrams have mass m , while the external states and the lines in the interior of the diagram are all massless. This is believed to be sufficient to regulate all IR divergences of planar scattering amplitudes.² The original SYM theory is then recovered by taking m small.

Using the Higgs regulator described above, the $\mathcal{N} = 4$ SYM planar four-gluon amplitude was computed at one and two loops in ref. [23] and at three loops in ref. [30], assuming that only integrals invariant under extended dual conformal symmetry contribute. It was shown that, at least through three loops, the Higgs-regulated four-gluon amplitude obeys an exponential ansatz

$$\begin{aligned} \log M_4(s, t) = & -\frac{1}{8}\gamma(a) \left[\log^2\left(\frac{s}{m^2}\right) + \log^2\left(\frac{t}{m^2}\right) \right] - \tilde{\mathcal{G}}_0(a) \left[\log\left(\frac{s}{m^2}\right) + \log\left(\frac{t}{m^2}\right) \right] \\ & + \frac{1}{8}\gamma(a) \left[\log^2\left(\frac{s}{t}\right) + \pi^2 \right] + \tilde{c}_4(a) + \mathcal{O}(m^2) \end{aligned} \quad (1.1)$$

analogous to the BDS ansatz in dimensional regularization. Here $M_4(s, t)$ is the ratio of the all-orders planar amplitude to the tree-level amplitude, $\gamma(a)$ is the cusp anomalous dimension [31], and $\tilde{\mathcal{G}}_0(a)$ and $\tilde{c}_4(a)$ are analogs of functions appearing in the BDS ansatz. One of the advantages of the Higgs-regulated ansatz (1.1) is that IR divergences take the form of logarithms of m^2 ; consequently, the L -loop amplitude may be computed by simply exponentiating $\log M_4(s, t)$ without regard for the $\mathcal{O}(m^2)$ terms since they continue to vanish as $m \rightarrow 0$ even when multiplied by logarithms of m^2 . Putting it another way, in order to test eq. (1.1) one need not compute any $\mathcal{O}(m^2)$ terms of the Higgs-regulated L -loop amplitudes because they cannot make any contribution to the IR-finite part of $\log M(s, t)$. This stands in stark contrast to dimensional regularization, where checking the BDS ansatz

¹Or rather the slightly stronger assumption (which holds in every known example) that every amplitude can be expressed in an integral basis in which each element is dual conformal invariant.

²More precisely, diagrams which cannot be rendered finite in this manner also cannot be rendered finite in off-shell regularization, and it is believed that such diagrams never contribute to the amplitude [8].

at each additional loop order requires recalculation of two more terms in the ϵ expansion of each lower loop integral.

One of the results of the current paper is to extend the computation of the Higgs-regulated four-gluon amplitude to four loops. Following the observed behavior through three loops, we assume that the Higgs-regulated four-loop amplitude can be expressed as the same linear combination of eight scalar integrals as the dimensionally-regulated amplitude. Specializing to the kinematic point $s = t$, we demonstrate that the result is consistent with the exponentiation of IR divergences built into the BDS ansatz (1.1), and we confirm, with significantly improved numerical precision, the value of the four-loop cusp anomalous dimension found in refs. [32, 33].

Taking the Regge limit $s \gg t$, the ansatz (1.1) implies that the Higgs-regulated four-gluon amplitude exhibits exact Regge behavior [8, 34–39]

$$M_4(s, t) = M_4(t, s) = \beta(t) \left(\frac{s}{m^2}\right)^{\alpha(t)-1} \tag{1.2}$$

where the all-loop-orders Regge trajectory is

$$\alpha(t) - 1 = -\frac{1}{4}\gamma(a) \log\left(\frac{t}{m^2}\right) - \tilde{\mathcal{G}}_0(a). \tag{1.3}$$

The coefficient of $\log t$, the cusp anomalous dimension, is independent of the IR regulator, while the constant part is scheme-dependent. In ref. [30], we verified that the Higgs-regulated four-gluon amplitude obeys eq. (1.2) through three-loop order, and in the current paper, we extend this to four loops.

Equation (1.1) implies that the L -loop amplitude has leading log (LL) expansion

$$\begin{aligned} M_4^{(L)} = & \frac{(-1)^L}{L!} \log^L\left(\frac{t}{m^2}\right) \log^L\left(\frac{s}{m^2}\right) \\ & + (-1)^{L-1} \left[\left(\frac{\pi^2}{2(L-1)!} - \frac{\pi^2}{6(L-2)!} \right) \log^{L-1}\left(\frac{t}{m^2}\right) \right. \\ & \quad \left. - \frac{\zeta_3}{(L-2)!} \log^{L-2}\left(\frac{t}{m^2}\right) \right] \log^{L-1}\left(\frac{s}{m^2}\right) \\ & + \mathcal{O}\left(\log^{L-2}\left(\frac{s}{m^2}\right)\right) \end{aligned} \tag{1.4}$$

where the LL $\log^L s$ term depends only on the lowest-order term $\gamma(a) = -4a + \mathcal{O}(a^2)$ of the cusp anomalous dimension, while the next-to-leading log (NLL) $\log^{L-1} s$ term depends on the $\mathcal{O}(a^2)$ terms of $\gamma(a)$ and $\tilde{\mathcal{G}}_0(a)$. We showed in ref. [30] that the LL term stems entirely from a single scalar diagram, the vertical ladder, in the Regge limit of the Higgs-regulated loop expansion.³ In this paper, we show that the NLL contribution to the L -loop

³There are two ways of taking the Regge limit of a Higgs-regulated amplitude. One can either (a) first take the limit $m^2 \ll s, t$, and then $s \gg t$, or (b) first take the limit $s \gg t, m^2$, and then $m^2 \ll t$. We demonstrated in ref. [30] that the amplitude is independent of the order of limits, at least through three loops. The Regge behavior of individual diagrams, however, can depend on the order in which the limits are taken. The dominance of vertical ladder diagrams is only valid in the Regge (b) limit, and the discussion in the text assumes this order of limits.

amplitude is given by the subleading term of the vertical ladder, together with the leading contributions from a set of $(L - 1)$ diagrams, consisting of vertical ladder diagrams with a single H-shaped insertion. We explicitly confirm this through five loops via a Mellin-Barnes computation, and present an argument (subject to certain reasonable assumptions) for its validity to all loops.

A second thrust of this paper is to consider higher-point amplitudes in Higgs regularization. We compute the Higgs-regulated five-gluon amplitude at one- and two-loops and establish the iterative relation

$$M_5^{(2)} = \frac{1}{2} \left(M_5^{(1)} \right)^2 + \sum_{i=1}^5 \left[\frac{\zeta_2}{4} \log^2 \left(\frac{s_i}{m^2} \right) + \frac{\zeta_3}{2} \log \left(\frac{s_i}{m^2} \right) \right] - \zeta_2 F_5^{(1)}(s_i) + \frac{5}{4} \zeta_4 + \mathcal{O}(m^2) \quad (1.5)$$

where

$$F_5^{(1)}(s_i) = \lim_{m^2 \rightarrow 0} \left[M_5^{(1)} + \frac{1}{4} \sum_{i=1}^5 \log^2 \left(\frac{s_i}{m^2} \right) \right] \quad (1.6)$$

is the IR-finite part of the one-loop amplitude, which is the same as in dimensional regularization, up to an additive constant. We argue that the parity-odd part of $M_5^{(2)}$ is at most $\mathcal{O}(m^2)$ in Higgs regularization.

Based on the iterative relation (1.5), we propose that the generalization of eq. (1.1) to the planar MHV n -gluon amplitude in Higgs regularization takes the form

$$\log M_n = \sum_{i=1}^n \left[-\frac{\gamma(a)}{16} \log^2 \left(\frac{s_i}{m^2} \right) - \frac{\tilde{\mathcal{G}}_0(a)}{2} \log \left(\frac{s_i}{m^2} \right) + \tilde{f}(a) \right] + \frac{1}{4} \gamma(a) F_n^{(1)} + \mathcal{R}_n + \tilde{C}(a) + \mathcal{O}(m^2) \quad (1.7)$$

with

$$\tilde{f}(a) = \frac{\pi^4}{180} a^2 + \mathcal{O}(a^3), \quad \tilde{C}(a) = -\frac{\pi^4}{72} a^2 + \mathcal{O}(a^3) \quad (1.8)$$

and \mathcal{R}_n vanishes for $n = 4$ and $n = 5$. For $n \geq 6$, we expect the remainder function \mathcal{R}_n to be equal to its counterpart in dimensional regularization.

Various Regge limits of the n -gluon amplitude for $n \geq 5$ can be defined (see, e.g., refs. [40, 41]). We consider the single and double Regge limits (in the Euclidean region) of the Higgs-regulated five-gluon amplitude up to two loops. In both of these cases, the double logarithm in $\log M_5$ cancels out, leaving single logarithmic dependence on the large kinematic variable.

In ref. [30], an alternative approach to the Regge limit for four-gluon amplitudes was considered by taking a different point on the Coulomb branch, involving two different masses. We extend this approach to single and double Regge limits of the five-gluon amplitude. In both cases, this alternative approach makes clear that $\log M_5$ should only have single logarithmic dependence on the kinematic variables because collinear divergences are absent. A similar approach can be taken for some, but not necessarily all, of the $n = 6$ Regge limits considered in refs. [40, 41].

The paper is organized as follows. In section 2 we study the four-gluon amplitude, presenting explicit results for all contributing four-loop integrals at the symmetric point $s = t$ and arguing that, to all loops, the NLL contribution to the amplitude in the Regge

limit is given by a small subset of all diagrams. In section 3 we turn our attention to the five-gluon amplitude at two loops, the evaluation of which leads to eq. (1.5). Section 4 contains a discussion of various Regge limits of Higgs-regulated amplitudes for $n \geq 5$, with emphasis on those features which differ from similar limits of dimensionally-regulated amplitudes. Section 5 summarizes our results, while various technical details can be found in three appendices.

2 The four-point amplitude

In ref. [23], it was suggested that the analog of the Bern-Dixon-Smirnov ansatz [12] for the planar four-point amplitude in Higgs regularization is

$$\begin{aligned} \log M_4(s, t) = & -\frac{1}{8}\gamma(a) \left[\log^2\left(\frac{s}{m^2}\right) + \log^2\left(\frac{t}{m^2}\right) \right] - \tilde{\mathcal{G}}_0(a) \left[\log\left(\frac{s}{m^2}\right) + \log\left(\frac{t}{m^2}\right) \right] \\ & + \frac{1}{8}\gamma(a) \left[\log^2\left(\frac{s}{t}\right) + \pi^2 \right] + \tilde{c}_4(a) + \mathcal{O}(m^2) \end{aligned} \quad (2.1)$$

where

$$\gamma(a) = \sum_{\ell=1}^{\infty} a^\ell \gamma^{(\ell)} = 4a - 4\zeta_2 a^2 + 22\zeta_4 a^3 + \mathcal{O}(a^4) \quad (2.2)$$

is the cusp anomalous dimension, and

$$\tilde{\mathcal{G}}_0(a) = -\zeta_3 a^2 + \mathcal{O}(a^3), \quad \tilde{c}_4(a) = \frac{\pi^4}{120} a^2 + \mathcal{O}(a^3) \quad (2.3)$$

are analogs of functions appearing in the BDS ansatz in dimensional regularization [12], but need not be identical since they are scheme-dependent [23]. Overlapping soft and collinear IR divergences are responsible for the double logarithms in eq. (2.1). The nontrivial content of eq. (2.1) is the statement about the finite terms; the IR singular terms of the amplitude are expected to obey eq. (2.1) on general field theory grounds (see refs. [42, 43]).

According to the assumption of dual conformal symmetry, the planar L -loop amplitude can be written as

$$M^{(L)} = \sum_I c(I) I \quad (2.4)$$

where the sum runs over all extended dual conformal integrals I , with some coefficients $c(I)$. In the case of the four-point amplitude, the coefficients are simply numbers. The set of loop integrals invariant under extended dual conformal symmetry is significantly smaller than that of generic loop integrals.

At two and three loops, the assumption (2.4), together with the infrared consistency conditions, leads to a result in agreement with the exponential ansatz (2.1), with the values (2.2), (2.3) and⁴ [30]

$$\tilde{\mathcal{G}}_0^{(3)} \approx 2.688870547851 \pm 6.5 \times 10^{-11}, \quad \tilde{c}_4^{(3)} \approx -9.24826993 \pm 9.6 \times 10^{-7}. \quad (2.5)$$

⁴In the course of the four-loop computation of the present paper we have improved the numerical accuracy of $\tilde{\mathcal{G}}_0^{(3)}$ and $\tilde{c}_4^{(3)}$ quoted in ref. [30]. Here we display the results with improved numerical accuracy.

If one assumes that these coefficients have transcendentality⁵ 5 and 6 respectively, one finds for them the probable analytic values⁶

$$\tilde{\mathcal{G}}_0^{(3)} = \frac{9}{2}\zeta_5 - \zeta_2\zeta_3, \quad \tilde{c}_4^{(3)} = -\frac{25}{4}\zeta_6 - 2\zeta_3^2 \quad (2.6)$$

using the PSLQ algorithm [44, 45].

The three-loop amplitude was computed [30] by assuming that

$$M_4^{(3)}(s, t) = -\frac{1}{8} \left[I_{3a}(s, t) + 2I_{3b}(s, t) \right] + (s \leftrightarrow t). \quad (2.7)$$

There are two additional dual conformal invariant three-loop integrals, I_{3c} and I_{3d} , with powers of m^2 in the numerator, but which have a finite $m \rightarrow 0$ limit. These could in principle contribute to the three-loop amplitude if the coefficients multiplying them are nonzero. In ref. [30], we showed that even in this case the exponential ansatz remains valid, provided that the coefficients $\tilde{\mathcal{G}}_0^{(3)}$ and $\tilde{c}_4^{(3)}$ are shifted accordingly.

2.1 Four-loop four-point amplitude

For the four-loop four-gluon amplitude, we will use the ansatz [32]

$$M_4^{(4)}(s, t) = \frac{1}{16} \left[I_{4a}(s, t) + 2I_{4b}(s, t) + 2I_{4c}(s, t) + I_{4d}(s, t) + 4I_{4e}(s, t) + 2I_{4f}(s, t) - 2I_{4d_2}(s, t) - \frac{1}{2}I_{f_2}(s, t) \right] + (s \leftrightarrow t) \quad (2.8)$$

where the individual integrals, shown in figure 1, are defined in dimensional regularization in ref. [32]. These integrals are all dual conformal invariant, and are straightforwardly rewritten in Higgs regularization, following refs. [23, 30]. For example, using dual coordinates [1] for convenience, we have

$$I_{4b}(s, t) = \int \frac{d^4x_a d^4x_b d^4x_c d^4x_d}{(i\pi^2)^4} \frac{x_{13}^2(x_{24}^2)^2(x_{1d}^2 + m^2)^2}{(x_{1a}^2 + m^2)(x_{1b}^2 + m^2)(x_{1c}^2 + m^2)(x_{2a}^2 + m^2)(x_{2d}^2 + m^2)} \times \frac{1}{(x_{3d}^2 + m^2)(x_{4d}^2 + m^2)(x_{4c}^2 + m^2)x_{ab}^2x_{bc}^2x_{ad}^2x_{bd}^2x_{cd}^2}. \quad (2.9)$$

Note that in I_{4d} there is no $+m^2$ term in the loop-dependent numerator, since it connects two internal integration points.

We have written down Mellin-Barnes representations for all eight integrals. This is easily done introducing the MB representation loop by loop [30, 46]. Interestingly, the dimensionality of most MB representations is one lower than the corresponding representation in dimensional regularization. At two and three loops, the opposite was the case.

⁵If we attribute a degree of transcendentality 0, 1, 1 and n , respectively to rational numbers, π , log and ζ_n , and define the transcendentality of a product to be additive, then the L -loop amplitude is expected to have uniform transcendentality $2L$.

⁶We thank Lance Dixon for suggesting this value of $\tilde{\mathcal{G}}_0^{(3)}$ to us.

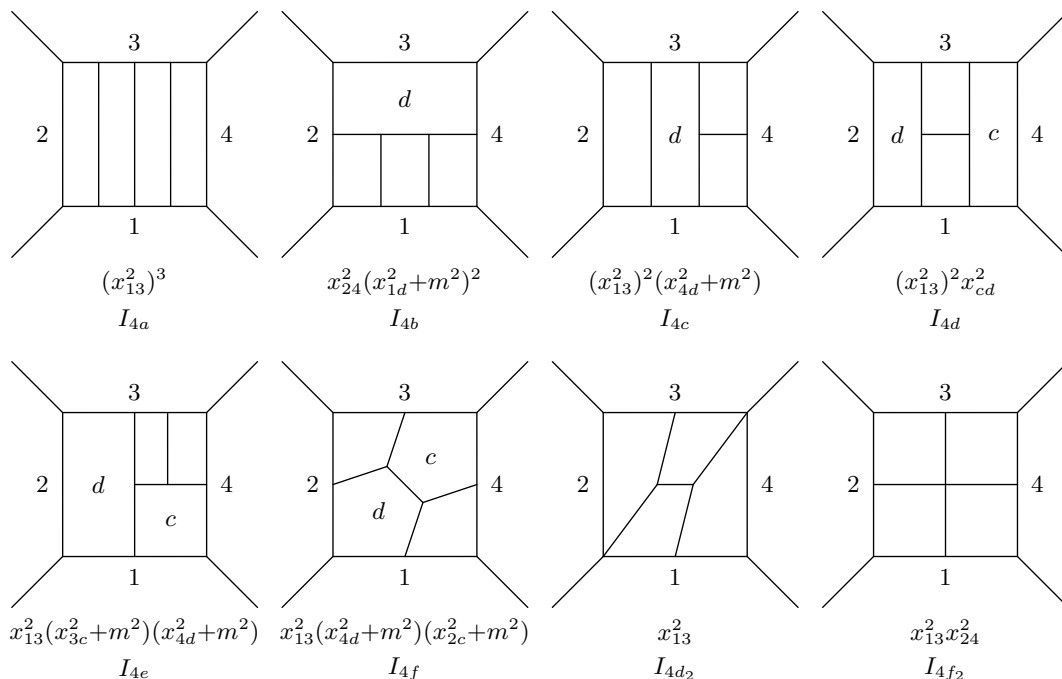


Figure 1. The eight diagrams contributing to the four-loop four-point amplitude. We use the standard dual variable notation, labeling the external faces by x_1 through x_4 and the internal faces by x_a through x_d . The former are related to the external momenta via $p_i = x_i - x_{i+1}$ (where i is understood mod 4) while the latter are each integrated with the measure $d^4x/(i\pi^2)$. Under each diagram is shown the numerator factor for the corresponding integral. To avoid clutter, we omit an overall factor of $x_{13}^2x_{24}^2 = st$ from each diagram (where $x_{ab} \equiv x_a - x_b$), and we do not label internal faces not appearing in numerator factors. As an illustrative example we demonstrate how to assemble all ingredients of the integral I_{4b} in eq. (2.9).

To make contact with the exponential ansatz (2.1), we will compute $M_4(s, t)$ at the symmetric point $s = t$. Defining $x = m^2/s = m^2/t$, the expression above becomes

$$M_4^{(4)}(x) = \frac{1}{16} \left[2I_{4a}(x) + 4I_{4b}(x) + 4I_{4c}(x) + 2I_{4d}(x) + 8I_{4e}(x) + 4I_{4f}(x) - 4I_{4d_2}(x) - I_{f_2}(x) \right]. \tag{2.10}$$

To evaluate these integrals, we proceed as in refs. [23, 30]. The starting point is a multi-dimensional MB representation depending on the parameter x . For simplicity, consider a one-dimensional MB integral

$$\int_{\beta-i\infty}^{\beta+i\infty} dz x^z f(z) \tag{2.11}$$

where typically $f(z)$ is a product of Γ functions, and $\beta < 0$. In principle, one could close the integration contour, say, on the right and obtain the answer as an infinite series arising from poles of the Γ functions in $f(z)$. However, since we are only interested in the $\log x$ terms as $x \rightarrow 0$, it is sufficient to deform the integration contour to positive values of $\text{Re}(z)$. The logarithms arise from taking residues at $z = 0$. In the case of multi-fold MB integrals, the above strategy can be iterated. We obtain expressions of the form

$\sum_{i=0}^6 b_i \log^{8-i} x + \mathcal{O}(\log x)$ using the Mathematica code *MBasymptotics* [47]. In general, the coefficients b_i still involve a (significantly lower) number of MB integrals, which we evaluate numerically using the code *MB* [48]. Denoting $L = \log x$, we find

$$I_{4a}(x) = \frac{1}{56}L^8 + \frac{8}{135}\pi^2L^6 - \frac{8}{15}\zeta_3L^5 - \frac{2}{27}\pi^4L^4 \quad (2.12)$$

$$+ \left(-\frac{32}{3}\zeta_2\zeta_3 - \frac{8}{3}\zeta_5\right)L^3 + (-162.26621838645 \pm 1.9 \times 10^{-10})L^2 + \mathcal{O}(L).$$

$$I_{4b}(x) = \frac{149}{5040}L^8 - \frac{1}{60}\pi^2L^6 - \frac{6}{5}\zeta_3L^5 + \frac{11}{72}\pi^4L^4 \quad (2.13)$$

$$+ \left(\frac{151}{3}\zeta_2\zeta_3 + \frac{247}{6}\zeta_5\right)L^3 + (525.46852427784 \pm 9.9 \times 10^{-10})L^2 + \mathcal{O}(L).$$

$$I_{4c}(x) = \frac{271}{10080}L^8 - \frac{2}{3}\zeta_3L^5 - \frac{11}{270}\pi^4L^4 \quad (2.14)$$

$$+ \left(-2\zeta_2\zeta_3 - \frac{127}{3}\zeta_5\right)L^3 + (-128.86933736 \pm 4.2 \times 10^{-7})L^2 + \mathcal{O}(L).$$

$$I_{4d}(x) = \frac{9}{560}L^8 + \frac{19}{270}\pi^2L^6 - \frac{4}{15}\zeta_3L^5 - \frac{19}{135}\pi^4L^4 \quad (2.15)$$

$$+ \left(-\frac{128}{3}\zeta_2\zeta_3 - 40\zeta_5\right)L^3 + (-710.51212126801 \pm 1.4 \times 10^{-10})L^2 + \mathcal{O}(L).$$

$$I_{4e}(x) = \frac{271}{10080}L^8 + \frac{1}{60}\pi^2L^6 - \frac{2}{3}\zeta_3L^5 - \frac{191}{2160}\pi^4L^4 \quad (2.16)$$

$$+ \left(-\frac{23}{6}\zeta_2\zeta_3 - \frac{335}{12}\zeta_5\right)L^3 + (222.7007725 \pm 1.8 \times 10^{-6})L^2 + \mathcal{O}(L).$$

$$I_{4f}(x) = \frac{199}{2520}L^8 - \frac{22}{135}\pi^2L^6 - \frac{12}{5}\zeta_3L^5 + \frac{17}{30}\pi^4L^4 \quad (2.17)$$

$$+ \left(68\zeta_2\zeta_3 + \frac{286}{3}\zeta_5\right)L^3 + (-117.32774717 \pm 1.8 \times 10^{-7})L^2 + \mathcal{O}(L).$$

$$I_{4d_2}(x) = -\frac{8}{15}\zeta_3L^5 + \frac{2}{45}\pi^4L^4 \quad (2.18)$$

$$+ \left(16\zeta_2\zeta_3 - \frac{16}{3}\zeta_5\right)L^3 + (180.37203096920 \pm 6.6 \times 10^{-10})L^2 + \mathcal{O}(L).$$

$$I_{4f_2}(x) = \frac{199}{1260}L^8 - \frac{44}{135}\pi^2L^6 - \frac{88}{15}\zeta_3L^5 + \frac{17}{15}\pi^4L^4 \quad (2.19)$$

$$+ \left(168\zeta_2\zeta_3 + \frac{700}{3}\zeta_5\right)L^3 + (324.1906414642 \pm 2.6 \times 10^{-9})L^2 + \mathcal{O}(L).$$

Summing up the contributions of the four-loop integrals computed above using eq. (2.10), we obtain

$$M_4^{(4)}(x) = \frac{1}{24}L^8 - \zeta_3L^5 + \frac{1}{60}\pi^4L^4 + (6\zeta_2\zeta_3 - 9\zeta_5)L^3 + (6.71603090 \pm 9.1 \times 10^{-7})L^2 + \mathcal{O}(L). \quad (2.20)$$

The coefficients of L^4 and L^3 in the expressions above were obtained numerically, so we cannot distinguish between rational and transcendental numbers. Nevertheless, motivated by the expectation that the result should have uniform transcendentality, we have replaced

the numerical values by their probable analytical equivalents. Specifically, we used the Mathematica implementation of the PSLQ algorithm to identify linear combinations of numbers with the correct degree of transcendentality that agree with our results within the numerical accuracy. It goes without saying that this does not constitute a proof that these expressions are necessarily correct. A guess for the numerical coefficient of the L^2 term is $-\frac{1}{2}\zeta_6 + 5\zeta_3^2$.

Exponentiation of the IR logarithms requires that

$$M_4^{(4)}(x) = \frac{1}{24}L^8 - \zeta_3 L^5 + \frac{1}{60}\pi^4 L^4 + \left(4\zeta_2\zeta_3 - 2\tilde{\mathcal{G}}_0^{(3)}\right)L^3 + \left(-\tilde{c}_4^{(3)} - \frac{1}{4}\gamma^{(4)} - \frac{13}{360}\pi^6 + 2\zeta_3^2\right)L^2 + \mathcal{O}(L) \quad (2.21)$$

where we have used the values of $\gamma(a)$, $\tilde{\mathcal{G}}_0(a)$, and $\tilde{c}_4(a)$ given in eqs. (2.2) and (2.3). There is complete agreement between eqs. (2.20) and (2.21). Comparing the coefficients of L^3 , we confirm the value $\tilde{\mathcal{G}}_0^{(3)} = \frac{9}{2}\zeta_5 - \zeta_2\zeta_3$ obtained at three loops by assuming that I_{3d} does not contribute. Comparing the coefficients of L^2 , we confirm the value $\tilde{c}_4^{(3)} = -\frac{25}{4}\zeta_6 - 2\zeta_3^2$ obtained at three loops by assuming that I_{3c} does not contribute, provided that the four-loop cusp anomalous dimension is given by

$$\gamma^{(4)} = -117.1788222 \pm 3.7 \times 10^{-6} \approx -4\zeta_2^3 - 24\zeta_2\zeta_4 - 4\zeta_3^2 - 50\zeta_6 \quad (2.22)$$

in perfect agreement with the result (also numerical) found in refs. [32, 33], and in agreement with the spin chain prediction from ref. [49]. It is noteworthy that our result (2.22) improves the numerical precision by two orders of magnitude compared to ref. [33] and by five orders of magnitude compared to ref. [32].⁷

Similar to the situation at three loops, there are 10 four-loop integrals (in addition to those shown in eq. (2.8)) that could in principle contribute to the four-loop amplitude, based solely on requiring dual conformal invariance [50]. As we have seen, however, our results are completely consistent with the absence of these additional integrals at three and four loops.

It is amusing that the coefficients appearing in the results for the individual integrals are rather complicated (e.g. the coefficients of the L^8 terms), yet they sum up to give the very simple result (2.20), as required by infrared consistency. This suggests there may exist a better organization of the calculation that avoids the complexity of the intermediate results.

2.2 Regge limit of the four-point function

The four-point amplitude (2.1) can be rewritten as

$$\log M_4 = -\frac{1}{4}\gamma(a)(\log v)(\log u) + \tilde{\mathcal{G}}_0(a)(\log u + \log v) + \frac{\pi^2}{8}\gamma(a) + \tilde{c}_4(a) + \mathcal{O}(m^2) \quad (2.23)$$

⁷The value (2.22) corresponds to $r = -1.99999892 \pm 6.3 \times 10^{-7}$ in the parameterization used in those references.

where $u = m^2/s$ and $v = m^2/t$. Note that $(\log u)^2$ and $(\log v)^2$ terms are absent, which is related to the Regge-exactness of the four-point amplitude. This can alternatively be interpreted as follows [30]. The Higgs-regulated amplitude can be computed at a different point in moduli space, where the diagrams contain internal lines with different masses m and M along the periphery, and external lines with mass $M - m$. By dual conformal invariance, the amplitude only depends on $u = m^2/s$ and $v = M^2/t$. The absence of $(\log m^2)^2$ terms in the amplitude can be understood as the absence of collinear divergences when massive (M) particles scatter by exchanging lighter (m) particles (with the mass of the lighter particles serving as an IR regulator).

We may exponentiate eq. (2.23), and expand the result in powers of the coupling a and of the Regge logarithms $\log u$. At L -loop order, the leading logarithm is $\log^L u$, NLL is $\log^{L-1} u$, etc. To LL and NLL order, the L -loop amplitude in the Regge limit is given by

$$\begin{aligned}
 M_4^{(L)} = & \left[\frac{1}{L!} (-\log v)^L \right] \log^L u \\
 & + \left[\left(\frac{\pi^2}{2(L-1)!} - \frac{\pi^2}{6(L-2)!} \right) (-\log v)^{L-1} - \frac{\zeta_3}{(L-2)!} (-\log v)^{L-2} \right] \log^{L-1} u \\
 & + \mathcal{O}(\log^{L-2} u)
 \end{aligned}
 \tag{2.24}$$

where we have used eqs. (2.2) and (2.3). In contrast to dimensional regularization, in Higgs regularization there is a single diagram, the vertical ladder $I_{La}(v, u)$ (see figure 2), that contributes⁸ to the LL term of the L -loop amplitude (2.24). In the LL limit, the vertical ladder factorizes into a product of (two-dimensional) bubble integrals (again see figure 2). Moreover, the LL, NLL, and NNLL contributions of the vertical ladder diagram were computed (cf. eq. (4.16) in ref. [30]) using the method of ref. [51]. Subtracting the vertical ladder contribution from the prediction (2.24) for the full amplitude, we obtain

$$M_4^{(L)} - \left(-\frac{1}{2} \right)^L I_{La}(v, u) = \frac{(-1)^L}{3(L-2)!} \log^{L-1} u [\log^{L+1} v + \pi^2 \log^{L-1} v + \mathcal{O}(v)] + \mathcal{O}(\log^{L-2} u).
 \tag{2.25}$$

From this, one sees that contributions from diagrams other than the vertical ladder are required at NLL order to obtain the expected amplitude in the Regge limit.

Rules for evaluating the leading $\log s$ behavior of multiloop integrals were summarized in refs. [51, 52]. One begins by identifying paths through the graph, which, when contracted to a point, split the diagram into two parts with a single vertex in common, and with p_1 and p_4 on one side and p_2 and p_3 on the other (for example, each of the rungs of the vertical ladder diagram). Paths of minimal length are called “d-lines” [53] or “t-paths” [54]. A scalar diagram containing m d-lines of length n goes as $\log^{m-1} s/s^n$ as $s \rightarrow \infty$. For example, the L -loop vertical ladder diagram contains $(L + 1)$ d-lines of length one, so the vertical ladder integral (multiplied by st^L to make it dual conformal invariant) goes as $\log^L s$, or equivalently $\log^L u$, as discussed above. All other L -loop diagrams contain at most $(L - 1)$ d-lines and hence *prima facie* give at most a $\log^{L-2} u$ contribution. For example, the four-loop diagrams $I_{4c}(v, u)$ and $I_{4d}(v, u)$ (see figure 1) each contain two d-lines of length one

⁸in the Regge (b) limit (see footnote 3).

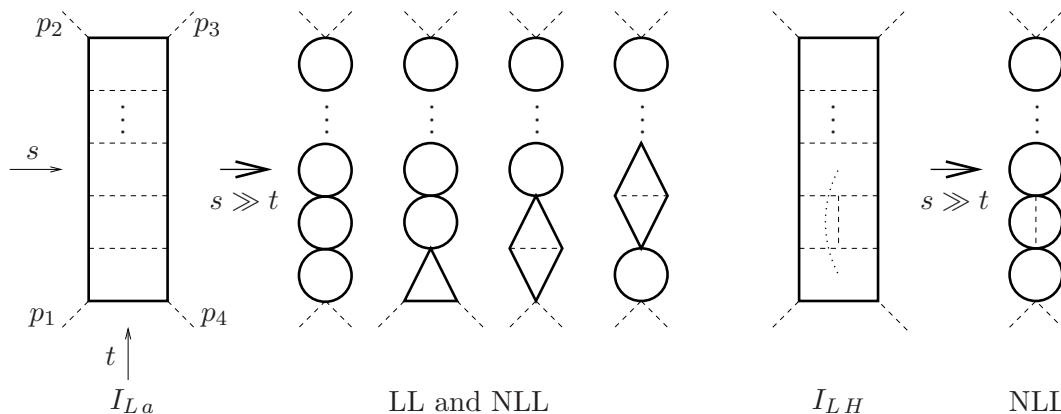


Figure 2. Factorization of the leading-log and next-to-leading-log contributions to the Regge limit $s \gg t$ of the L -loop vertical ladder integral $I_{La}(v, u)$ into simpler integrals. Factorization of the NLL contribution of the vertical ladder integral with H-shaped insertion I_{LH} . The dotted line indicates a loop-momentum-dependent numerator.

and *prima facie* go as $\log u$. (These diagrams also contain two paths of length two, which are not minimal and therefore do not contribute.)

The MB calculation summarized in appendix A, however, shows that both of these diagrams go as $\log^3 u$, two powers higher than expected. This is because the d-line rules given above only apply to scalar diagrams with no non-trivial (i.e., loop-momentum-dependent) numerator factors. The presence of numerator factors, which are required for the loop integrations next to the H-shaped insertion to have the correct dual conformal weight, can increase the leading power of $\log u$ of the diagram. The reader may ascertain from the results of appendix A that diagrams with no nontrivial numerator factors have the $\log u$ dependence predicted by the d-line rules, whereas those with numerator factors can have a stronger $\log u$ dependence.

We show in appendix B that when an H-shaped insertion in a vertical ladder diagram is accompanied by a numerator factor, the two lines of length two constituting the sides of the H are effectively promoted to length one, increasing the d-line count by two. In particular, an L -loop vertical ladder diagram with a single H-shaped insertion I_{LH} (see figure 2), which *prima facie* would go as $\log^{L-3} u$, actually goes as $\log^{L-1} u$ due to its numerator factors, and thus contributes to the amplitude at NLL order. A calculation in appendix B further shows that, subject to reasonable assumptions, the leading log contribution of the integral I_{LH} factorizes as

$$I_{LH} = \frac{(-1)^{L-1}}{(L-1)!} \log^{L-1} u \times K(v)^{L-2} \times K'(v) + \mathcal{O}(\log^{L-2} u), \quad (2.26)$$

where $K(v)$ and $K'(v)$ correspond to the two-dimensional bubble and two-loop bubble diagrams shown in figure 2 (see ref. [30] for further discussion). Taking v small, we have

$$\begin{aligned} K(v) &= -2 \log v + \mathcal{O}(v), \\ K'(v) &= -\frac{4}{3} \log^3 v - \frac{4}{3} \pi^2 \log v + \mathcal{O}(v). \end{aligned} \quad (2.27)$$

Note that eq. (2.26) implies that the position where the H-shaped insertion is made into the vertical ladder integral is unimportant at NLL order, i.e. all such integrals give the same NLL contribution.

At two loops, I_{LH} is just the horizontal ladder $I_{2a}(u, v)$. At three loops, I_{LH} is the tennis court diagram $I_{3b}(u, v)$. In ref. [30], it was shown that the leading contribution of these diagrams is precisely given by eq. (2.26). At four loops, the three I_{LH} diagrams are given by $I_{4c}(v, u)$, its flipped version, and $I_{4d}(v, u)$. The results for these integrals found in appendix A are also in agreement with eq. (2.26) and, moreover, all other four-loop diagrams contribute at most to NNLL. Finally, we have verified eq. (2.26) at five loops as well using the integrals given in ref. [5].

At L -loop order there are $(L-1)$ vertical ladder diagrams containing a single H -shaped insertion, so that the total contribution to the amplitude of the vertical ladders with one H-shaped insertion is (multiplying the contributions by $(-1/2)^L$)

$$\left(-\frac{1}{2}\right)^L (L-1)I_{LH} = \frac{(-1)^L}{3(L-2)!} \log^{L-1} u [\log^{L+1} v + \pi^2 \log^{L-1} v + \mathcal{O}(v)] + \mathcal{O}(\log^{L-2} u) \tag{2.28}$$

which precisely matches the result (2.25) expected from the exponential ansatz.

In summary, we have shown that in Higgs regularization, the NLL contribution to the four-gluon amplitude in the Regge limit is given by a small set of diagrams: the vertical ladders and the vertical ladders with one H-shaped insertion. We confirmed this through five loops by direct evaluation of the integrals, and we gave an argument that this holds to all loop orders.

3 The five-point amplitude

In this section, we direct our attention to the two-loop $n = 5$ point amplitude of $\mathcal{N} = 4$ SYM theory, which is of interest for several reasons. It serves as a further instructive application of the Higgs mechanism to regulate infrared divergences, and confirms the universality of the exponential structure of IR singularities of n -point amplitudes in massless gauge theories (which is usually studied in dimensional regularization; for example, see refs. [42, 43]). We also establish an iterative relation at two loops, which is the exact analog of the five-point iterative relation in dimensional regularization [55, 56]. This allows us to write an all-loop ansatz for n -point amplitudes in Higgs regularization, analogous to the BDS ansatz in dimensional regularization, whose content is that the IR-finite part of the amplitudes also exponentiates. Of course the separation between IR-divergent and IR-finite terms is not unique since one could always add a constant to one while subtracting the same constant from the other. Knowledge of the four-point amplitude alone does not give enough information to resolve this ambiguity in a natural way, but after computing the five-point amplitude, we will be able to determine a unique way of writing the universal IR-divergent part of the Higgs-regulated scattering amplitude for any n .

As in ref. [30] we evade a Feynman diagram calculation by beginning with the ansatz that Higgs-regulated five-point loop amplitudes (normalized, as usual, by dividing by the corresponding tree amplitudes) can be expressed as linear combinations of all possible dual

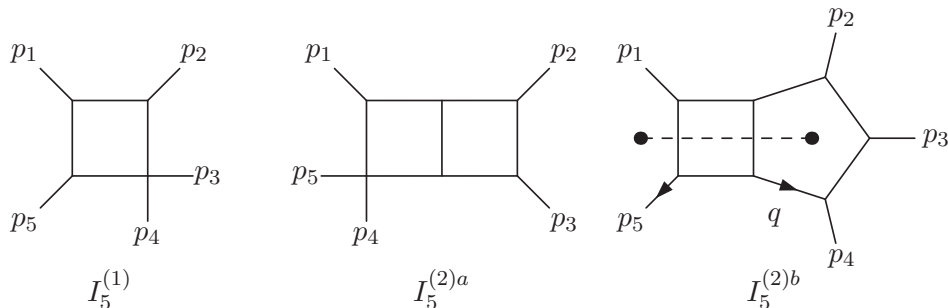


Figure 3. Dual conformal scalar integrals contributing to the five-particle amplitude at one and two loops. The dashed line indicates that the integral contains the loop-momentum-dependent numerator factor $(q + p_5)^2 + m^2$.

conformally invariant scalar integrals. At one loop there is a unique integral $I_5^{(1)}(s_i)$ (see figure 3) that can appear in the ansatz

$$M_5^{(1)} = -\frac{1}{4} \sum_{\text{cyclic}} s_1 s_5 I_5^{(1)}(s_i) + \mathcal{O}(m^2), \quad (3.1)$$

where $+\mathcal{O}(m^2)$ stands for potential parity-odd terms (see below),

$$s_i = (p_i + p_{i+1})^2, \quad i = 1, \dots, 5 \quad (3.2)$$

(with $p_6 \equiv p_1$), and the sum in eq. (3.1) runs over the five cyclic permutations of the external momenta p_i . The small m^2 expansion of $I_5^{(1)}(s_i)$ is given in appendix C. After summing over cyclic permutations, the one-loop amplitude simplifies to

$$M_5^{(1)} = \sum_{i=1}^5 \left[-\frac{1}{4} \log^2 \left(\frac{s_i}{m^2} \right) \right] + F_5^{(1)} + \mathcal{O}(m^2) \quad (3.3)$$

where the corresponding finite remainder $F_5^{(1)}$ is given by⁹

$$F_5^{(1)} = -\frac{1}{4} \sum_{i=1}^5 \left[\log \left(\frac{s_i}{s_{i+1}} \right) \log \left(\frac{s_{i-1}}{s_{i+2}} \right) - \frac{\pi^2}{3} \right] \quad (3.4)$$

with $s_{i+5} = s_i$.

At two loops there are two dual conformal invariant scalar integrals that contribute to the amplitude: the double box $I_5^{(2)a}(s_i)$ and the pentagon-box $I_5^{(2)b}(s_i)$ with a numerator factor involving the pentagon loop momentum (see figure 3). The coefficients of these integrals in the amplitude $M_5^{(2)}(s_i)$ are determined by the consistency of infrared singularities, leading to the ansatz

$$M_5^{(2)} = -\frac{1}{8} \sum_{\text{cyclic}} \left[s_1 s_2^2 I_5^{(2)a}(s_i) + s_3^2 s_4 I_5^{(2)a}(s_{6-i}) + s_2 s_3 s_5 I_5^{(2)b}(s_i) \right] + \mathcal{O}(m^2), \quad (3.5)$$

⁹Recently it has been shown [58, 59] that, when expressed in momentum-twistor variables, the expression in eqs. (3.3) and (3.4) computes the volume of a 4-simplex in AdS₅ with 5 (regulated) points on the boundary.

where, as in the four-point calculation, the relative numerical coefficients of each diagram are precisely the same as in dimensional regularization.

Out of abundance of caution we have included $+\mathcal{O}(m^2)$ in both eqs. (3.5) and (3.1) in order to encapsulate possible parity-odd terms. In dimensional regularization, $M_5^{(2)}$ has a non-vanishing parity-odd contribution starting at $\mathcal{O}(\epsilon^{-1})$. The parity-odd part of $\log M_5$, however, is $\mathcal{O}(\epsilon)$ at one- and two-loop order [55–57] due to the non-trivial cancellation of parity-odd terms in $M_5^{(2)}$ and $-\frac{1}{2}(M_5^{(1)})^2$, which also has a contribution starting at $\mathcal{O}(\epsilon^{-1})$. The vanishing of the parity-odd contribution to the Higgs-regulated amplitude $M_5^{(2)}$, together with the fact that terms that vanish as $m \rightarrow 0$ are not required to compute $\log M_5$ in Higgs regularization, implies that the parity-odd contribution to $\log M_5$ is $\mathcal{O}(m^2)$ at one and two loops.

The small m^2 expansions of $I_5^{(2)a}(s_i)$ and $I_5^{(2)b}(s_i)$ are given in appendix C. After summing over cyclic permutations, we find

$$M_5^{(2)} = \frac{1}{2} \left(M_5^{(1)} \right)^2 + \sum_{i=1}^5 \left[\frac{\zeta_2}{4} \log^2 \left(\frac{s_i}{m^2} \right) + \frac{\zeta_3}{2} \log \left(\frac{s_i}{m^2} \right) - \frac{\zeta_2}{4} \log^2 \left(\frac{s_i}{s_{i+1}} \right) + \frac{\zeta_2}{4} \log^2 \left(\frac{s_i}{s_{i+2}} \right) - \zeta_4 \right] + \mathcal{O}(m^2). \quad (3.6)$$

Using the identity

$$\sum_{i=1}^5 \log \left(\frac{s_i}{s_{i+3}} \right) \log \left(\frac{s_{i+1}}{s_{i+2}} \right) = \sum_{i=1}^5 \left[2 \log \left(\frac{s_i}{m^2} \right) \log \left(\frac{s_{i+1}}{m^2} \right) - 2 \log \left(\frac{s_i}{m^2} \right) \log \left(\frac{s_{i+2}}{m^2} \right) \right] \quad (3.7)$$

we may rewrite this as

$$M_5^{(2)} - \frac{1}{2} \left(M_5^{(1)} \right)^2 = \sum_{i=1}^5 \left[\frac{\zeta_2}{4} \log^2 \left(\frac{s_i}{m^2} \right) + \frac{\zeta_3}{2} \log \left(\frac{s_i}{m^2} \right) \right] - \zeta_2 F_5^{(1)} + \tilde{c}_5^{(2)} + \mathcal{O}(m^2) \quad (3.8)$$

where $\tilde{c}_5^{(2)} = \frac{5}{4}\zeta_4$ and $F_5^{(1)}(s_i)$ is given in eq. (3.4). Equation (3.8) is analogous to the two-loop five-point iterative relation of refs. [55, 56].

It is instructive to rewrite the one- and two-loop four-point amplitudes in a form similar to eqs. (3.3) and (3.8). Using eq. (2.1), with $s = s_1 = s_3$ and $t = s_2 = s_4$ for four-particle kinematics, we have

$$M_4^{(1)} = \sum_{i=1}^4 \left[-\frac{1}{4} \log^2 \left(\frac{s_i}{m^2} \right) \right] + F_4^{(1)} + \mathcal{O}(m^2), \quad (3.9)$$

$$M_4^{(2)} - \frac{1}{2} \left(M_4^{(1)} \right)^2 = \sum_{i=1}^4 \left[\frac{\zeta_2}{4} \log^2 \left(\frac{s_i}{m^2} \right) + \frac{\zeta_3}{2} \log \left(\frac{s_i}{m^2} \right) \right] - \zeta_2 F_4^{(1)} + \tilde{c}_4^{(2)} \quad (3.10)$$

where $\tilde{c}_4^{(2)} = \frac{3}{4}\zeta_4$ and

$$F_4^{(1)} = \frac{1}{8} \sum_{i=1}^4 \left[\log^2 \left(\frac{s_i}{s_{i+1}} \right) + \pi^2 \right]. \quad (3.11)$$

By re-expressing the constants in eqs. (3.8) and (3.10) as

$$\tilde{c}_n^{(2)} = \frac{(2n-5)}{4} \zeta_4 \tag{3.12}$$

we may combine eqs. (3.8) and (3.10) into

$$M_n^{(2)} - \frac{1}{2} \left(M_n^{(1)} \right)^2 = \sum_{i=1}^n \left[\frac{\zeta_2}{4} \log^2 \left(\frac{s_i}{m^2} \right) + \frac{\zeta_3}{2} \log \left(\frac{s_i}{m^2} \right) + \frac{\zeta_4}{2} \right] - \zeta_2 F_n^{(1)} - \frac{5}{4} \zeta_4 + \mathcal{O}(m^2), \tag{3.13}$$

$n = 4, 5.$

Note that the common infrared divergence term

$$\sum_{i=1}^n \left[\frac{\zeta_2}{4} \log^2 \left(\frac{s_i}{m^2} \right) + \frac{\zeta_3}{2} \log \left(\frac{s_i}{m^2} \right) + \frac{\zeta_4}{2} \right] \tag{3.14}$$

resembles the form expected from dimensional regularization [42, 43, 60]:

$$- [\zeta_2 + \zeta_3 \epsilon + \zeta_4 \epsilon^2] M_n^{(1)}(2\epsilon). \tag{3.15}$$

It would be interesting to understand more precisely the relation between these two forms of the infrared divergences, perhaps along the lines of ref. [61].¹⁰

Armed with the above ingredients we are now in a position to pose the n -point generalization of eq. (2.1) as

$$\begin{aligned} \log M_n &= \sum_{i=1}^n \left[-\frac{\gamma(a)}{16} \log^2 \left(\frac{s_i}{m^2} \right) - \frac{\tilde{\mathcal{G}}_0(a)}{2} \log \left(\frac{s_i}{m^2} \right) + \tilde{f}(a) \right] \\ &+ \frac{1}{4} \gamma(a) F_n^{(1)} + \mathcal{R}_n + \tilde{C}(a) + \mathcal{O}(m^2) \end{aligned} \tag{3.16}$$

where

$$\tilde{f}(a) = \frac{\zeta_4}{2} a^2 + \mathcal{O}(a^3), \quad \tilde{C}(a) = -\frac{5\zeta_4}{4} a^2 + \mathcal{O}(a^3) \tag{3.17}$$

and the remainder function \mathcal{R}_n vanishes for $n = 4$ and $n = 5$.

We can then proceed by defining the Higgs regularization analogs of the IR-finite functions F_n introduced in ref. [12] by subtracting the universal infrared singularities from the logarithm of the amplitude

$$F_n = \lim_{m^2 \rightarrow 0} \left(\log M_n - \sum_{i=1}^n \left[-\frac{\gamma(a)}{16} \log^2 \left(\frac{s_i}{m^2} \right) - \frac{\tilde{\mathcal{G}}_0(a)}{2} \log \left(\frac{s_i}{m^2} \right) + \tilde{f}(a) \right] \right). \tag{3.18}$$

The precise forms of the one-loop functions (3.4) and (3.11) and the two-loop functions

$$\begin{aligned} F_4^{(2)} &= \sum_{i=1}^4 \left[-\frac{\zeta_2}{8} \log^2 \left(\frac{s_i}{s_{i+1}} \right) - \frac{35\zeta_4}{16} \right], \\ F_5^{(2)} &= \sum_{i=1}^5 \left[-\frac{\zeta_2}{4} \log^2 \left(\frac{s_i}{s_{i+1}} \right) + \frac{\zeta_2}{4} \log^2 \left(\frac{s_i}{s_{i+2}} \right) - \frac{3\zeta_4}{2} \right] \end{aligned} \tag{3.19}$$

¹⁰We are grateful to S. Moch for discussion and correspondence on this question.

differ (by additive constants) from the corresponding expressions in dimensional regularization, which may be found in ref. [12]. Through two loops, however, the $n = 4$ and $n = 5$ IR-finite functions satisfy a similar iterative relation

$$F_n = \frac{1}{4}\gamma(a)F_n^{(1)} + \tilde{C}(a) + \mathcal{O}(a^3), \quad n = 4, 5. \quad (3.20)$$

While the constants $\tilde{\mathcal{G}}_0(a)$ and $\tilde{c}_n(a)$ defined above take different values in Higgs and in dimensional regularization, it is fascinating to note that the two-loop value of $\tilde{C}(a)$ in eq. (3.16) is identical to the corresponding value in dimensional regularization [60]. Perhaps this is a coincidence, or perhaps it has a deeper explanation, especially in light of the fact that the same value appears yet again in the finite part of the two-loop lightlike polygon Wilson loop after appropriate subtraction of UV divergences [62].

For $n \geq 6$, we expect that the “remainder” function \mathcal{R}_n in eq. (3.16) is non-trivial, just as in the corresponding formula in dimensional regularization [15, 16]. However it is natural to expect \mathcal{R}_n to take the same value in Higgs regularization as it does in dimensional regularization. This is because the remainder function is an infrared-finite, dual conformally invariant quantity (as required by the dual conformal Ward identity), so it constitutes a good “observable” of SYM theory. The 6-particle remainder function at two loops was first computed numerically in ref. [15], where agreement with the corresponding remainder function for lightlike hexagon Wilson loops [16, 63] was established, and an analytic expression has been given more recently in refs. [19–21].

4 Regge limits

In this section we discuss a number of features of the Regge limits of Higgs-regulated amplitudes for $n \geq 5$. As emphasized in footnote 3 such limits may be taken in two different orders: limits (a) where all m_i^2 are first taken to be much smaller than all kinematical invariants, and subsequently a Regge limit is taken, and limits (b) where the Regge limits are taken first with various fixed kinematic invariants and fixed masses m_i^2 , which are subsequently taken to be much smaller than the fixed kinematic invariants. The Regge behavior of individual diagrams can depend on the order, (a) or (b), in which these limits are taken.

4.1 The five-point amplitude

For the purposes of discussing the Regge limits of the five-gluon amplitude, we adopt the following parameterization of the kinematical invariants [40]

$$\begin{aligned} s &= (p_1 + p_2)^2, & t_1 &= (p_2 + p_3)^2, & s_1 &= (p_3 + p_4)^2, \\ s_2 &= (p_4 + p_5)^2, & t_2 &= (p_5 + p_1)^2, & s &= s_1 s_2 / \kappa. \end{aligned} \quad (4.1)$$

We will consider two different limits of these invariants, as defined in ref. [40]:

$$\textit{Single Regge limit:} \quad s \rightarrow \infty, \quad s_1 \rightarrow \infty, \quad \kappa, s_2, t_1, t_2 \text{ fixed}, \quad (4.2)$$

$$\textit{Double Regge limit:} \quad s \rightarrow \infty, \quad s_1 \rightarrow \infty, s_2 \rightarrow \infty \quad \kappa, t_1, t_2 \text{ fixed}. \quad (4.3)$$

In the following two sections, we will consider the Regge limits (a) and (b) for the five-point amplitude. We will see that, at least through two loops, the amplitude is the same in both limits.

4.2 Regge (a) limits for $n = 5$

If we wish to take Regge limit (a) of the five-gluon amplitude, we can start with the conjectured ansatz (3.16), in which the small m^2 limit has already been taken. In terms of the parameters (4.1), eq. (3.16) for $n = 5$ takes the form

$$\begin{aligned} \log M_5 = & \omega(t_1) \log\left(\frac{s_1}{m^2}\right) + \omega(t_2) \log\left(\frac{s_2}{m^2}\right) \\ & + \frac{1}{16} \gamma(a) \left[-\log^2\left(\frac{t_1}{t_2}\right) - \log^2\left(\frac{\kappa}{m^2}\right) + 2 \log\left(\frac{\kappa}{m^2}\right) \log\left(\frac{t_1 t_2}{m^4}\right) \right] \\ & - \frac{1}{2} \tilde{\mathcal{G}}_0 \left[\log\left(\frac{t_1}{m^2}\right) + \log\left(\frac{t_2}{m^2}\right) - \log\left(\frac{\kappa}{m^2}\right) \right] + \mathcal{O}(m^2) \end{aligned} \quad (4.4)$$

where

$$\omega(t) = \alpha(t) - 1 = -\frac{1}{4} \gamma(a) \log\left(\frac{t}{m^2}\right) - \tilde{\mathcal{G}}_0(a) \quad (4.5)$$

is the same trajectory as in the four-point function (1.3). Equation (4.4) is equivalent to [14, 40]

$$M_5 = \left(\frac{s_1}{m^2}\right)^{\omega(t_1)} \left(\frac{s_2}{m^2}\right)^{\omega(t_2)} F(t_1, t_2, \kappa), \quad (4.6)$$

which exhibits the expected factorization. From eq. (4.6) it is straightforward to take the Regge limit to obtain the following expressions, separating the Regge behavior from the fixed term:

$$\textit{Single Regge (a) limit:} \quad M_5 \longrightarrow \left(\frac{s_1}{m^2}\right)^{\omega(t_1)} \left[\left(\frac{s_2}{m^2}\right)^{\omega(t_2)} F(t_1, t_2, \kappa) \right], \quad (4.7)$$

$$\textit{Double Regge (a) limit:} \quad M_5 \longrightarrow \left(\frac{s_1}{m^2}\right)^{\omega(t_1)} \left(\frac{s_2}{m^2}\right)^{\omega(t_2)} [F(t_1, t_2, \kappa)]. \quad (4.8)$$

Equations (4.7) and (4.8) have the same form as in ref. [40], but with a different value for the constant term in the trajectory function (4.5), and a different $F(t_1, t_2, \kappa)$ due to the difference between eq. (4.4) and the analogous BDS result.

4.3 Regge (b) limits for $n = 5$

To obtain the Regge (b) limits of the five-point amplitude, one must start with scalar integrals with finite m , take the Regge limit first, and only afterwards take m small. We have evaluated the five-point one- and two-loop diagrams in this way and have obtained results identical to eq. (4.7) in the single Regge limit and to eq. (4.8) in the double Regge limit. Hence, at least to two-loop order, the amplitude is independent¹¹ of the order in which the Regge limit is taken (even though the individual diagrams are not).

¹¹In an “unphysical” Regge limit $s \rightarrow \infty$ with s_1, s_2, t_1, t_2 fixed, described on p. 177 of ref. [51], the one-loop amplitude does depend on the order of limits, yielding $\log^2 s$ dependence in the Regge (a) limit, as can be seen from eq. (4.4), but $\log s$ dependence in the Regge (b) limit.

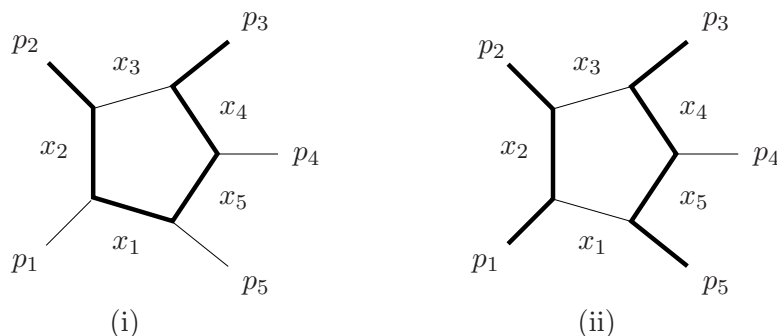


Figure 4. Two-mass configurations illustrating the (i) single and (ii) double Regge (b) limits for the five-point amplitude. Fat and thin lines along the periphery denote particles of mass M and m respectively. Fat and thin exterior lines denote particles of mass $M - m$ and 0 respectively.

In ref. [30], an alternative approach to the Regge (b) limits was applied to explain the absence of double logarithms in the Regge limit of the four-gluon amplitude. We can do the same for various Regge (b) limits of five-gluon amplitudes. Consider the theory at a different point on the Coulomb branch, where the scalar diagrams have internal lines with variable masses along the periphery (and vanishing masses in the interior). Let m_i be the mass of the line(s) connecting p_{i-1} and p_i . The masses of the external lines are given by $p_i^2 = -(m_i - m_{i+1})^2$. Due to dual conformal symmetry, the amplitude depends only on the dual conformal invariants

$$u_{i,i+2} = \frac{m_i m_{i+2}}{(p_i + p_{i+1})^2 + (m_i - m_{i+2})^2}. \tag{4.9}$$

By making various choices for m_i , we can reproduce the single and double Regge limits.

Single Regge (b) limit. By making the choice $m_3 = m$, and $m_i = M$ for $i \neq 3$, we have

$$u_{13} = \frac{Mm}{s + (M - m)^2}, \quad u_{24} = \frac{M^2}{t_1}, \quad u_{35} = \frac{Mm}{s_1 + (M - m)^2}, \quad u_{41} = \frac{M^2}{s_2}, \quad u_{52} = \frac{M^2}{t_1}. \tag{4.10}$$

Then taking the limit $m \ll M$ yields $u_{13}, u_{35} \ll u_{24}, u_{41}, u_{52}$, which is equivalent to the single Regge limit (4.2). The resulting diagrams (e.g., see figure 4(i)) cannot have collinear divergences because the massless external lines never connect to the light mass internal lines. The amplitude therefore has at most a simple $\log m$ IR divergence, which corresponds to $\log u_{35}$ (or $\log u_{13}$) and therefore to a simple $\log s_1$ dependence in the single Regge limit, in agreement with eq. (4.4).

Double Regge (b) limit. By choosing $m_1 = m_3 = m$, and $m_2 = m_4 = m_5 = M$, we have

$$u_{13} = \frac{m^2}{s}, \quad u_{24} = \frac{M^2}{t_1}, \quad u_{35} = \frac{Mm}{s_1 + (M - m)^2}, \quad u_{41} = \frac{Mm}{s_2 + (M - m)^2}, \quad u_{52} = \frac{M^2}{t_1}. \tag{4.11}$$

Taking the limit $m \ll M$ yields $u_{13} \ll u_{35}, u_{41} \ll u_{24}, u_{52}$, which is equivalent to the double Regge limit (4.3). Again, none of the diagrams that contribute to the amplitude in

this limit has collinear divergences (e.g., see figure 4(ii)), hence the amplitude has at most a simple $\log m$ IR divergence, which corresponds to $\log u_{35}$ or $\log u_{41}$, and therefore to a simple $\log s_1$ or $\log s_2$ dependence in the double Regge limit, in agreement with eq. (4.4).

4.4 Regge (a) limits for $n \geq 6$

To consider various Regge (a) limits of $n \geq 6$ amplitudes, we may start with the conjectured ansatz (3.16), in which the small m^2 limit has already been taken.

For $n = 4$ and $n = 5$ we have seen that $F_n^{(1)}$, the IR-finite part of the one-loop amplitude, has the same dependence on kinematic variables (up to an additive constant) as the corresponding function in dimensional regularization. Any difference in the form of $F_n^{(1)}$ for $n \geq 6$ between Higgs-regulated amplitudes and dimensionally-regulated amplitudes should be dual conformal invariant, and therefore a function of dual cross-ratios. Any such function remains finite in Euclidean Regge limits [40]. Similarly, the remainder function \mathcal{R}_n in either Higgs regularization or in dimensional regularization remains finite in Euclidean Regge limits, as discussed in section 7 of ref. [40]. Therefore, the Regge (a) limits of Higgs-regulated amplitudes are equivalent to the Euclidean Regge limits of dimensionally-regulated amplitudes discussed in refs. [40, 41], but with the Regge trajectories given by eq. (4.5). Similarly the Regge vertex functions will be analogous to those in ref. [40], but will differ in detail due to the difference in the IR-regulator scheme.

It is possible that \mathcal{R}_n could contribute to Regge limits in the physical region, as these may involve contributions which do not remain finite. However, it is known that there are difficulties in continuing M_n ($n \geq 6$) from the Euclidean to the physical region [14, 41, 64]. These same difficulties would be present for Higgs-regulated amplitudes, so we do not consider these latter limits further.

In conclusion, there are no important differences between the Regge (a) limits of Higgs-regulated vs. dimensionally-regulated n -gluon amplitudes.

4.5 Regge limit (b) for $n = 6$

We have not attempted to compute the amplitudes for $n \geq 6$ in any of the Regge (b) limits defined in [40, 41] to ascertain whether they are equivalent to the Regge (a) limits discussed in the previous subsection.

However, we would like to point out that the analysis of some of these limits could be facilitated by considering Higgs-regulated amplitudes at various points on the Coulomb branch. Let m_i be the mass of the lines on the periphery of a diagram connecting external lines p_{i-1} and p_i , with vanishing masses in the interior. We consider points on the Coulomb branch involving just two distinct mass assignments m and M (with $m \ll M$).

There are four inequivalent configurations (for six-point amplitudes) that yield at most single logarithmic dependence on the IR-regulator mass m . (These are configurations where no two adjacent m_i are equal to m .) We can classify these configurations according to the number of lines with the small mass m .

One line with small mass. If we set $m_1 = m$ and m_2 through m_6 equal to M , then none of the massless external lines are attached to the line(s) on the periphery with mass m . Hence there are no collinear divergences, and the amplitude only goes as $\log m$.

Two lines with small mass. There are two possibilities involving two lines with small mass. The first one consists in setting $m_1 = m_3 = m$, with the remaining masses given by M . The second consist in setting $m_1 = m_4 = m$, with the remaining masses given by M . The latter corresponds to the Mueller-Regge limit discussed in section 7.4 of ref. [41].

Three lines with small mass. If the external masses alternate between m and M (i.e. $m_1 = m_3 = m_5 = m$ and $m_2 = m_4 = m_6 = M$), one obtains the poly-Regge limit of section 7.3 of ref. [41].

No two-mass set-up has been found to give the single Regge limit or helicity pole limit.

5 Summary

In this paper we have continued the program of computing higher-loop $\mathcal{N} = 4$ SYM planar n -gluon amplitudes and testing various conjectures using the Higgs regulator scheme proposed in ref. [23] and further developed in ref. [30]. Specifically, we have extended the analysis to four loops for the four-gluon amplitude, and to two loops for the five-gluon amplitude, using Mellin-Barnes techniques to evaluate the integrals. We have assumed that only scalar diagrams invariant under extended dual conformal symmetry contribute to the amplitudes, and with the same numerical coefficients as in dimensional regularization. Although one has no *a priori* guarantee that the set of diagrams contributing to the amplitude in one IR-regulator scheme coincides with the set in another scheme, all the results we obtained using this assumption are consistent with the universal IR-divergence structure of massless gauge theories and also with the conjectured all-loop ansatz (1.7) for the IR-finite part. For all cases considered, we have verified that the IR-finite parts of the logarithm of the amplitudes have the same dependence on kinematic variables as the corresponding functions in dimensionally-regulated amplitudes (up to overall additive constants, which we determine).

We have also extended the study of the Regge behavior of Higgs-regulated amplitudes which was begun in ref. [30]. The Regge (a) limits (in which the masses are first taken much smaller than all kinematic invariants, and then the Regge limit of kinematic variables is applied) can be understood by simply taking the kinematic limits of the ansatz (1.7), in which $\mathcal{O}(m^2)$ terms are already neglected. Various (a) type limits are discussed for $n \geq 5$ which give essentially the same results as those from the dimensionally-regulated BDS ansatz, but with different expressions for the gluon trajectory and Regge vertices resulting from the different regulator scheme.

To study Regge (b) limits (in which the kinematical limits are first taken with fixed regulator masses, which are subsequently taken to be much smaller than the fixed kinematic invariants) one must evaluate the Regge limits of the individual diagrams contributing to the amplitudes. In the Regge (b) limit, certain classes of diagrams are dominant, whereas in the Regge (a) limit no single class of diagrams dominates. In ref. [30], it was shown

that the leading-log approximation of the four-gluon amplitude is dominated to all loop orders by the sum of vertical ladder diagrams only. In this paper, we showed that the next-to-leading-log approximation depends only on the vertical ladder diagrams, together with the class of vertical ladder diagrams with a single H-shaped insertion.

One way of analyzing Regge (b) limits of diagrams is to go to a different point on the Coulomb branch involving several different masses. Examples are given for several Regge limits of $n = 5$ and $n = 6$ amplitudes using two different masses, although we have not been able to obtain all Regge (b) limits using two-mass configurations on the Coulomb branch. Although the Regge (a) and Regge (b) limits of individual diagrams differ, we have found that the full amplitudes are independent of the order of limits in the cases that we have considered.

The results of this paper show that the Higgs regulator for planar $\mathcal{N} = 4$ SYM amplitudes continues to exhibit a number of practical and conceptual advantages compared to other regulators, the first signs of which were observed in ref. [23, 30]. On the practical side, the Higgs regulated multi-loop integrals we have encountered so far have proven quite a bit simpler to evaluate than their counterparts in dimensional regularization. One consequence of this is that we have been able to compute the four-loop cusp anomalous dimension with numerical precision five orders of magnitude greater than ref. [32] and two orders of magnitude greater than ref. [33]. The crucial conceptual advantage of the Higgs regulator is that it preserves the remarkable (extended) dual conformal symmetry which has recently played such an important role in unlocking the hidden structure of SYM amplitudes. While dimensional regularization seems completely at odds with modern (inherently four-dimensional) twistor-space methods, it is greatly encouraging that the Higgs regulator can be very naturally implemented in momentum twistor space, as seen for example in the beautiful recent results of ref. [58, 59], which we suspect are just the tip of the iceberg.

Acknowledgments

It is a pleasure to thank S. Moch, C.-I. Tan and A. Volovich for discussions and correspondence. J.H. is grateful to Brown University and to the Institute for Advanced Study, where part of this work was done, for hospitality.

A Regge limits of four-loop four-point integrals

In this appendix, we list the results for the Regge (b) limit of the each of the four-loop integrals that contribute to the four-loop amplitude. For compactness, we employ the notation $\{a_1, \dots, a_n\} \equiv \sum_{m=1}^n a_m \log^{n-m} v + \mathcal{O}(v)$.

$$I_{4a}(s, t) = \log u \left\{ \frac{8}{315}, 0, \frac{8}{45}\pi^2, 0, \frac{56}{135}\pi^4, 0, 252.30\dots, \text{const} \right\} + \mathcal{O}(\log^0 u). \tag{A.1}$$

$$I_{4a}(t, s) = \log^4 u \left\{ \frac{2}{3}, 0, 0, 0 \right\} + \log^3 u \left\{ -\frac{8}{3}, 0, -\frac{8}{3}\pi^2, -8\zeta_3, 0, 0 \right\} \tag{A.2}$$

$$\begin{aligned}
& + \log^2 u \left\{ \frac{214}{45}, 0, \frac{100}{9}\pi^2, \frac{64}{3}\zeta_3, \frac{154}{45}\pi^4, 183.07\dots, 11.55\dots \right\} \\
& + \log u \left\{ -\frac{1352}{315}, 0, -\frac{736}{45}\pi^2, -\frac{68}{3}\zeta_3, -\frac{608}{45}\pi^4, -580.84\dots, -1536.93\dots, \text{const} \right\} \\
& + \mathcal{O}(\log^0 u).
\end{aligned}$$

$$\begin{aligned}
I_{4b}(s, t) &= \log^2 u \left\{ \frac{4}{15}, 0, \frac{8}{9}\pi^2, 0, \frac{28}{45}\pi^4, 0, 0 \right\} \tag{A.3} \\
& + \log u \left\{ -\frac{257}{630}, 0, -\frac{101}{45}\pi^2, -\frac{16}{3}\zeta_3, -\frac{424}{135}\pi^4, -88.16\dots, -940.02\dots, \text{const} \right\} \\
& + \mathcal{O}(\log^0 u).
\end{aligned}$$

$$I_{4b}(t, s) = \log u \left\{ \frac{8}{63}, 0, \frac{16}{45}\pi^2, 0, \frac{8}{27}\pi^4, 0, 65.11\dots, \text{const} \right\} + \mathcal{O}(\log^0 u). \tag{A.4}$$

$$I_{4c}(s, t) = \log u \left\{ \frac{16}{315}, 0, \frac{8}{45}\pi^2, 0, \frac{32}{135}\pi^4, 0, 105.80\dots, \text{const} \right\} + \mathcal{O}(\log^0 u). \tag{A.5}$$

$$\begin{aligned}
I_{4c}(t, s) &= \log^3 u \left\{ \frac{8}{9}, 0, \frac{8}{9}\pi^2, 0, 0, 0 \right\} \tag{A.6} \\
& + \log^2 u \left\{ -\frac{121}{45}, 0, -\frac{56}{9}\pi^2, -\frac{32}{3}\zeta_3, -\frac{32}{15}\pi^4, -56.52\dots, 0 \right\} \\
& + \log u \left\{ \frac{1963}{630}, 0, \frac{539}{45}\pi^2, \frac{62}{3}\zeta_3, \frac{1478}{135}\pi^4, 622.32\dots, 1619.96\dots, \text{const} \right\} \\
& + \mathcal{O}(\log^0 u).
\end{aligned}$$

$$I_{4d}(s, t) = \log u \left\{ \frac{8}{315}, 0, \frac{8}{45}\pi^2, 0, \frac{56}{135}\pi^4, 0, 252.30\dots, \text{const} \right\} + \mathcal{O}(\log^0 u). \tag{A.7}$$

$$\begin{aligned}
I_{4d}(t, s) &= \log^3 u \left\{ \frac{8}{9}, 0, \frac{8}{9}\pi^2, 0, 0, 0 \right\} \tag{A.8} \\
& + \log^2 u \left\{ -\frac{44}{15}, 0, -\frac{52}{9}\pi^2, -8\zeta_3, -\frac{22}{9}\pi^4, -49.77\dots, 0 \right\} \\
& + \log u \left\{ \frac{1132}{315}, 0, 12\pi^2, \frac{56}{3}\zeta_3, \frac{428}{45}\pi^4, -191.36\dots, 863.63\dots, \text{const} \right\} \\
& + \mathcal{O}(\log^0 u).
\end{aligned}$$

$$I_{4e}(s, t) = \log u \left\{ \frac{8}{105}, 0, \frac{16}{45}\pi^2, 0, \frac{56}{135}\pi^4, 0, 130.22\dots, \text{const} \right\} + \mathcal{O}(\log^0 u). \tag{A.9}$$

$$\begin{aligned}
I_{4e}(t, s) &= \log^2 u \left\{ \frac{8}{15}, 0, \frac{8}{9}\pi^2, 0, \frac{16}{45}\pi^4, 0, 0 \right\} \tag{A.10} \\
& + \log u \left\{ -\frac{223}{210}, 0, -\frac{143}{45}\pi^2, -\frac{16}{3}\zeta_3, -\frac{22}{9}\pi^4, -49.77\dots, -258.40\dots, \text{const} \right\} \\
& + \mathcal{O}(\log^0 u).
\end{aligned}$$

$$I_{4f}(s, t) = \log u \left\{ \frac{16}{45}, 0, \frac{32}{45}\pi^2, -\frac{4}{3}\zeta_3, \frac{2}{5}\pi^4, -39.93\dots, 41.35\dots, \text{const} \right\} + \mathcal{O}(\log^0 u). \tag{A.11}$$

$$\begin{aligned}
I_{4f}(t, s) &= \log^2 u \left\{ \frac{8}{9}, 0, \frac{16}{9}\pi^2, 0, \frac{8}{9}\pi^4, 0, 0 \right\} \\
&+ \log u \left\{ -\frac{484}{315}, 0, -\frac{268}{45}\pi^2, -12\zeta_3, -\frac{734}{135}\pi^4, -103.20\dots, -907.47\dots, \text{const} \right\} \\
&+ \mathcal{O}(\log^0 u).
\end{aligned} \tag{A.12}$$

$$I_{4d_2}(s, t) = \log u \left\{ 0, 0, 0, -\frac{4}{3}\zeta_3, \frac{2}{45}\pi^4, -39.93\dots, 41.34\dots, \text{const} \right\} + \mathcal{O}(\log^0 u). \tag{A.13}$$

$$I_{4d_2}(t, s) = \log u \left\{ 0, 0, 0, -\frac{4}{3}\zeta_3, \frac{2}{15}\pi^4, -9.84\dots, 28.48\dots, \text{const} \right\} + \mathcal{O}(\log^0 u). \tag{A.14}$$

$$\begin{aligned}
I_{4f_2}(s, t) &= \log^2 u \left\{ \frac{8}{9}, 0, \frac{16}{9}\pi^2, 0, \frac{8}{9}\pi^4, 0, 0 \right\} \\
&+ \log u \left\{ -\frac{124}{105}, 0, -\frac{236}{45}\pi^2, -16\zeta_3, -\frac{136}{27}\pi^4, -109.95\dots, -935.95\dots, \text{const} \right\} \\
&+ \mathcal{O}(\log^0 u).
\end{aligned} \tag{A.15}$$

$$I_{4f_2}(t, s) = I_{4f_2}(s, t). \tag{A.16}$$

B Regge limit of the L -loop ladder with H -insertion

In this appendix, we evaluate the leading log contribution (in the limit of large s) of the dual conformal invariant L -loop vertical ladder diagram with one H-shaped insertion, I_{LH} , described in section 2.2.

We begin by considering an $(L - 1)$ -loop vertical ladder diagram, with the external regions labeled by x_1 through x_4 (where $s = x_{13}^2$ and $t = x_{24}^2$), and the loops labeled by x_i , with $i = 5, \dots, L + 4$ (see figure 5(i)). We replace the j th loop with a horizontal double loop, converting it into an L -loop diagram, as shown in figure 5(ii). By dual conformal invariance, this diagram must be accompanied by a factor of

$$x_{13}^2 x_{24}^{2(L-1)} x_{j-1, j+1}^2. \tag{B.1}$$

We now perform the integration over the double box. Its Feynman parameterization is

$$I_{\text{double box}} = \int_0^1 d\alpha_0 d\alpha_1 d\alpha_2 d\beta_1 d\beta_2 d\gamma_1 d\gamma_2 \frac{2A \delta(\alpha_0 + \alpha_1 + \alpha_2 + \delta_1 + \delta_2 - 1)}{(D + m^2\sigma A)^3} \tag{B.2}$$

where

$$\begin{aligned}
D &= D_{24}t + D_{j-1, j+1}P_{j-1, j+1} + D_{j-1, 2}P_{j-1, 2} + D_{j+1, 2}P_{j+1, 2} + D_{j-1, 4}P_{j-1, 4} + D_{j+1, 4}P_{j+1, 4} \\
A &= \alpha_0\alpha_1 + \alpha_0\alpha_2 + \alpha_1\alpha_2 + \alpha_0\delta_1 + \alpha_1(\delta_1 + \delta_2) + \alpha_2\delta_2 + \delta_1\delta_2 \\
\sigma &= \alpha_0 + \alpha_2 \\
\delta_i &= \beta_i + \gamma_i
\end{aligned} \tag{B.3}$$

with $P_{ij} \equiv x_{ij}^2 \equiv (x_i - x_j)^2$.

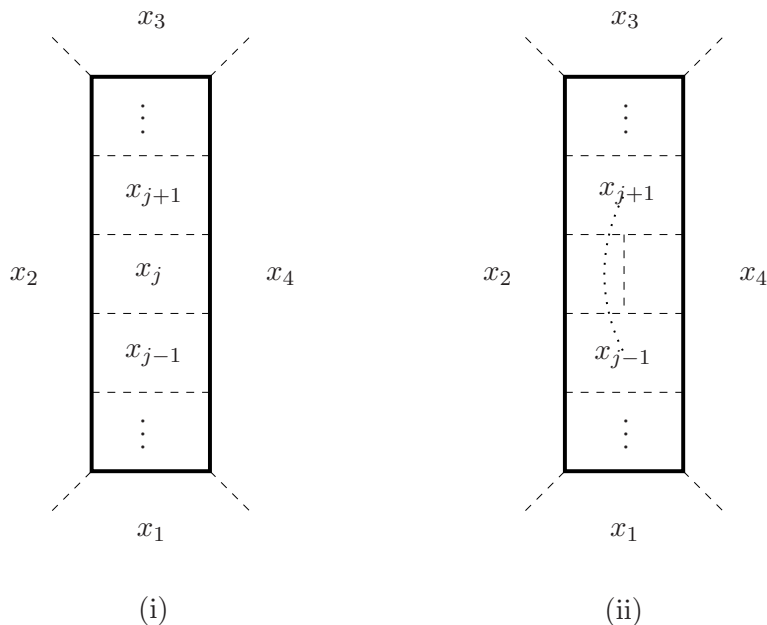


Figure 5. (i) Vertical ladder diagram and (ii) vertical ladder with H-shaped insertion (with numerator factor indicated by a dotted line) whose leading log contributions are computed in this appendix.

The coefficients of P_{ik} in eq. (B.3) are given by

$$\begin{aligned}
 D_{24} &= \alpha_0 \alpha_1 \alpha_2, & D_{j-1,j+1} &= (\alpha_2 + \delta_2) \beta_1 \gamma_1 + (\alpha_0 + \delta_1) \beta_2 \gamma_2 + \alpha_1 (\beta_1 + \beta_2) (\gamma_1 + \gamma_2), \\
 D_{j-1,2} &= \alpha_0 (\alpha_1 \beta_1 + \alpha_2 \beta_1 + \alpha_1 \beta_2 + \delta_2 \beta_1), & D_{j+1,2} &= \alpha_0 (\alpha_1 \gamma_1 + \alpha_2 \gamma_1 + \alpha_1 \gamma_2 + \delta_2 \gamma_1), \\
 D_{j-1,4} &= \alpha_2 (\alpha_1 \beta_2 + \alpha_0 \beta_2 + \alpha_1 \beta_1 + \delta_1 \beta_2), & D_{j+1,4} &= \alpha_2 (\alpha_1 \gamma_2 + \alpha_0 \gamma_2 + \alpha_1 \gamma_1 + \delta_1 \gamma_2).
 \end{aligned}
 \tag{B.4}$$

If the double box is inserted at one of the ends of the vertical ladder, the expression for σ in eq. (B.3) will contain additional terms $\beta_1 + \beta_2$ or $\gamma_1 + \gamma_2$, but the results below will be unaffected by this change.

We assume, following section 8 of ref. [65], that the asymptotic behavior of multiloop integrals is dominated by a region in the space of the loop momenta that can be described by a set of nested inequalities. In our specific case, those inequalities imply that the leading $s \rightarrow \infty$ behavior of I_{LH} comes from the region where $P_{j-1,j+1}$ is large (i.e. a nonzero fraction of s) with the other P_{ik} appearing in eq. (B.3) remaining finite. This in turn implies that the main contribution to the subintegral (B.2) arises from the part of parameter space where $D_{j-1,j+1}$, the coefficient of $P_{j-1,j+1}$, is small. This region may be identified by parameterizing [66]

$$\beta_1 = \rho_1 \zeta_1, \quad \beta_2 = \rho_1 \bar{\zeta}_1, \quad \gamma_1 = \rho_2 \zeta_2, \quad \gamma_2 = \rho_2 \bar{\zeta}_2
 \tag{B.5}$$

where ζ_i runs from 0 to 1, and $\bar{\zeta}_i \equiv 1 - \zeta_i$. In terms of these parameters, the main contribution to the subintegral comes from the region where ρ_1 and ρ_2 are both small.

Retaining only the lowest order terms in A and D ,

$$\begin{aligned}
 A &= \alpha_0\alpha_1 + \alpha_0\alpha_2 + \alpha_1\alpha_2 + \mathcal{O}(\rho_i), & (B.6) \\
 D_{24} &= \alpha_0\alpha_1\alpha_2, & D_{j-1,j+1} = \rho_1\rho_2(\alpha_1 + \alpha_2\zeta_1\zeta_2 + \alpha_0\bar{\zeta}_1\bar{\zeta}_2) + \mathcal{O}(\rho^3), \\
 D_{j-1,2} &= \rho_1\alpha_0(\alpha_1 + \alpha_2\zeta_1) + \mathcal{O}(\rho_1^2), & D_{j+1,2} = \rho_2\alpha_0(\alpha_1 + \alpha_2\zeta_2) + \mathcal{O}(\rho_2^2), \\
 D_{j-1,4} &= \rho_1\alpha_2(\alpha_1 + \alpha_0\bar{\zeta}_1) + \mathcal{O}(\rho_1^2), & D_{j+1,4} = \rho_2\alpha_2(\alpha_1 + \alpha_0\bar{\zeta}_2) + \mathcal{O}(\rho_2^2)
 \end{aligned}$$

we may approximate the term in the denominator of eq. (B.2) as

$$D + m^2\sigma A \approx \Gamma_0\rho_1\rho_2 + \Gamma_1\rho_1 + \Gamma_2\rho_2 + \Gamma_3 \quad (B.7)$$

with

$$\begin{aligned}
 \Gamma_0 &= (\alpha_1 + \alpha_2\zeta_1\zeta_2 + \alpha_0\bar{\zeta}_1\bar{\zeta}_2)P_{j-1,j+1} \\
 \Gamma_1 &= \alpha_0(\alpha_1 + \alpha_2\zeta_1)P_{j-1,2} + \alpha_2(\alpha_1 + \alpha_0\bar{\zeta}_1)P_{j-1,4} \\
 \Gamma_2 &= \alpha_0(\alpha_1 + \alpha_2\zeta_2)P_{j+1,2} + \alpha_2(\alpha_1 + \alpha_0\bar{\zeta}_2)P_{j+1,4} \\
 \Gamma_3 &= \alpha_0\alpha_1\alpha_2t + (\alpha_0\alpha_1 + \alpha_0\alpha_2 + \alpha_1\alpha_2)(\alpha_0 + \alpha_2)m^2. & (B.8)
 \end{aligned}$$

In the large s limit, $\Gamma_0 \gg \Gamma_1 \sim \Gamma_2 \sim \Gamma_3$. Inserting eq. (B.7) into eq. (B.2), we may approximate the integral as [51]

$$I_{\text{double box}} \approx \int_0^1 d\alpha_0 d\alpha_1 d\alpha_2 \delta(\alpha_0 + \alpha_1 + \alpha_2 - 1) (\alpha_0\alpha_1 + \alpha_0\alpha_2 + \alpha_1\alpha_2) \int_0^1 d\zeta_1 d\zeta_2 J \quad (B.9)$$

with

$$J = \int_0^{\eta_1} d\rho_1 \int_0^{\eta_2} d\rho_2 \frac{2\rho_1\rho_2}{(\Gamma_0\rho_1\rho_2 + \Gamma_1\rho_1 + \Gamma_2\rho_2 + \Gamma_3)^3} \quad (B.10)$$

where the factors of ρ_i in the numerator result from the Jacobian in the change of variables. To capture the dominant behavior of the integral, we only need integrate ρ_1 and ρ_2 over a small region near the origin; the exact values of the upper limits η_1, η_2 are unimportant but are both taken to be $\ll 1$ to justify the neglect of higher order terms in ρ_i in the integrand and the dropping of δ_i from the argument of the Dirac delta function. The integral over ρ_i yields

$$J \approx \frac{\Gamma_3}{(\Gamma_0\Gamma_3 - \Gamma_1\Gamma_2)^2} \log \left(\frac{(\Gamma_0\eta_1\eta_2 + \Gamma_1\eta_1 + \Gamma_2\eta_2 + \Gamma_3)\Gamma_3}{(\Gamma_1\eta_1 + \Gamma_3)(\Gamma_2\eta_2 + \Gamma_3)} \right) \approx \frac{1}{\Gamma_0^2\Gamma_3} \log \Gamma_0 \quad (B.11)$$

where in the last step we used the approximation $\Gamma_0 \gg \Gamma_1 \sim \Gamma_2 \sim \Gamma_3$. Inserting eq. (B.11) into eq. (B.9), we find

$$I_{\text{double box}} \approx \frac{K'(v)}{t} \frac{\log P_{j-1,j+1}}{P_{j-1,j+1}^2} \quad (B.12)$$

where $v = m^2/t$ and

$$\begin{aligned}
 K'(v) &= \int_0^1 d\alpha_0 d\alpha_1 d\alpha_2 & (B.13) \\
 &\times \int_0^1 d\zeta_1 d\zeta_2 \frac{\delta(\alpha_0 + \alpha_1 + \alpha_2 - 1) (\alpha_0\alpha_1 + \alpha_0\alpha_2 + \alpha_1\alpha_2)}{(\alpha_1 + \alpha_2\zeta_1\zeta_2 + \alpha_0\bar{\zeta}_1\bar{\zeta}_2)^2 [\alpha_0\alpha_1\alpha_2 + (\alpha_0\alpha_1 + \alpha_0\alpha_2 + \alpha_1\alpha_2)(\alpha_0 + \alpha_2)v]}.
 \end{aligned}$$

Thus in the $s \rightarrow \infty$ limit, integrating out the double box is equivalent to inserting eq. (B.12) into the remaining integral.

We observe that $K'(v)$ may be identified as the coefficient of $(\log s)/(s^2 t)$ in the two-loop horizontal ladder diagram in the asymptotic $s \rightarrow \infty$ regime. When v is small, $K'(v)$ can be explicitly evaluated to give [30]

$$K'(v) = -\frac{4}{3} \log^3 v - \frac{4}{3} \pi^2 \log v + \mathcal{O}(v). \quad (\text{B.14})$$

Next we consider an $(L-1)$ -loop vertical ladder integral $I_{L-1,a}$, supplemented with a numerator factor of $x_{13} x_{24}^{L-1}$ to make it dual conformal invariant. Consider just the subintegral over the j th loop

$$I_{\text{single box}} = \int_0^1 d\alpha_0 d\alpha_1 d\beta_1 d\gamma_1 \frac{\delta(\alpha_0 + \alpha_1 + \beta_1 + \gamma_1 - 1)}{(\Gamma_0 \beta_1 \gamma_1 + \Gamma_1 \beta_1 + \Gamma_2 \gamma_1 + \Gamma_3)^2} \quad (\text{B.15})$$

where

$$\begin{aligned} \Gamma_0 &= P_{j-1,j+1} \\ \Gamma_1 &= \alpha_0 P_{j-1,2} + \alpha_1 P_{j-1,4} \\ \Gamma_2 &= \alpha_0 P_{j+1,2} + \alpha_1 P_{j+1,4} \\ \Gamma_3 &= \alpha_0 \alpha_1 t + m^2 (\alpha_0 + \alpha_1). \end{aligned} \quad (\text{B.16})$$

As before, the leading $s \rightarrow \infty$ behavior of the vertical ladder integral comes from the region of loop momentum space where $P_{j-1,j+1}$ is much larger than the other P_{ik} , i.e., where $\Gamma_0 \gg \Gamma_1 \sim \Gamma_2 \sim \Gamma_3$. This in turn implies that the main contribution to the subintegral (B.15) arises from the region of parameter space where β_1 and γ_1 are both small. We may therefore approximate eq. (B.15) as

$$I_{\text{single box}} \approx \int_0^1 d\alpha_0 d\alpha_1 \delta(\alpha_0 + \alpha_1 - 1) \int_0^{\eta_1} d\beta_1 \int_0^{\eta_2} d\gamma_1 \frac{1}{(\Gamma_0 \beta_1 \gamma_1 + \Gamma_1 \beta_1 + \Gamma_2 \gamma_1 + \Gamma_3)^2}. \quad (\text{B.17})$$

The integral over β_1 and γ_1 yields

$$\frac{1}{\Gamma_0 \Gamma_3 - \Gamma_1 \Gamma_2} \log \left(\frac{(\Gamma_0 \eta_1 \eta_2 + \Gamma_1 \eta_1 + \Gamma_2 \eta_2 + \Gamma_3) \Gamma_3}{(\Gamma_1 \eta_1 + \Gamma_3)(\Gamma_2 \eta_2 + \Gamma_3)} \right) \approx \frac{1}{\Gamma_0 \Gamma_3} \log \Gamma_0 \quad (\text{B.18})$$

where in the last step we have used the approximation $\Gamma_0 \gg \Gamma_1, \Gamma_2, \Gamma_3$. Hence we obtain for the subintegral

$$I_{\text{single box}} \approx \frac{K(v)}{t} \frac{\log P_{j-1,j+1}}{P_{j-1,j+1}} \quad \text{where} \quad K(v) = \int_0^1 d\alpha_0 d\alpha_1 \frac{\delta(\alpha_0 + \alpha_1 - 1)}{\alpha_0 \alpha_1 + v}. \quad (\text{B.19})$$

Thus, in the $s \rightarrow \infty$ limit, integrating out a single box is equivalent to the insertion of eq. (B.19) in the remaining integral. Here $K(v)$ is just the coefficient of $(\log s)/(st)$ in the one-loop box diagram in the asymptotic $s \rightarrow \infty$ regime. When v is small, it can be explicitly evaluated to give

$$K(v) = -2 \log v + \mathcal{O}(v). \quad (\text{B.20})$$

We note that eqs. (B.12) and (B.19) are quite similar, except that the powers of $P_{j-1,j+1}$ in the denominators differ. This reflects the fact that the two d-lines (described in section 2.2) for the double box have length two whereas those for the single box only have unit length. Recall, however, that dual conformal invariance implies that the I_{LH} diagram comes with a factor of $P_{j-1,j+1}$ in the numerator (B.1), which cancels one of the factors in the denominator of eq. (B.12), “promoting” the d-lines to length one. (This in turn raises the number of powers of $\log s$ in the asymptotic behavior of the integral by two.)

Taking into account all the numerator factors, we see that the quotient of I_{LH} and $I_{L-1,a}$ is given by

$$\frac{I_{LH}}{I_{L-1,a}} = \frac{K'(v)}{K(v)}. \tag{B.21}$$

We know however from ref. [30, 51] that

$$\lim_{u \ll v} I_{L-1,a} = \frac{(-1)^{L-1}}{(L-1)!} K(v)^{L-1} \log^{L-1} u + \dots \tag{B.22}$$

from which we conclude that

$$\lim_{u \ll v} I_{LH} = \frac{(-1)^{L-1}}{(L-1)!} K(v)^{L-2} K'(v) \log^{L-1} u + \dots \tag{B.23}$$

which is used in the main body of the paper in eq. (2.26).

C Five-point integrals

In this appendix, we give small- m^2 expansions for the Higgs-regulated one- and two-loop five-point integrals shown in figure 3.

The one-loop box integral $I_5^{(1)}$ has the small m^2 expansion

$$\begin{aligned} s_1 s_5 I_5^{(1)} &= \log^2 m^2 - 2 \log \left(\frac{s_1 s_5}{s_3} \right) \log m^2 \\ &+ 2 \log s_1 \log s_5 - \log^2 s_3 - 2 \text{Li}_2 \left(1 - \frac{s_3}{s_1} \right) - 2 \text{Li}_2 \left(1 - \frac{s_3}{s_5} \right) - \frac{\pi^2}{3}. \end{aligned} \tag{C.1}$$

Assembling everything into dimensionless ratios s_i/m^2 , the result can be stated more succinctly as

$$s_1 s_5 I_5^{(1)} \approx 2 \log \left(\frac{s_1}{m^2} \right) \log \left(\frac{s_5}{m^2} \right) - \log^2 \left(\frac{s_3}{m^2} \right) - 2 \text{Li}_2 \left(1 - \frac{s_3}{s_1} \right) - 2 \text{Li}_2 \left(1 - \frac{s_3}{s_5} \right) - \frac{\pi^2}{3} + \mathcal{O}(m^2). \tag{C.2}$$

The double-box integral $I_5^{(2)a}$ has the small m^2 expansion

$$\begin{aligned}
s_1 s_2^2 I^{(2)a} = & -\frac{1}{4} \log^4 m^2 + \log\left(\frac{s_1 s_2}{s_4}\right) \log^3 m^2 \\
& + \left[-\frac{3}{2} \log^2\left(\frac{s_1 s_2}{s_4}\right) - 2 \text{Li}_2\left(1 - \frac{s_2}{s_4}\right) - \frac{\pi^2}{6} \right] \log^2 m^2 \\
& + \left[\log^3\left(\frac{s_1 s_2}{s_4}\right) - \frac{\pi^2}{3} \log\left(\frac{s_1}{s_2 s_4}\right) + 4 \log\left(\frac{s_1}{s_4}\right) \text{Li}_2\left(1 - \frac{s_1}{s_4}\right) \right. \\
& + 4 \log\left(\frac{s_1 s_2}{s_4}\right) \text{Li}_2\left(1 - \frac{s_2}{s_4}\right) - 4 \text{Li}_3\left(1 - \frac{s_2}{s_4}\right) + 8 H_{011}\left(1 - \frac{s_1}{s_4}\right) - 4 \zeta_3 \left. \right] \log m^2 \\
& + \mathcal{O}(\log^0 m^2),
\end{aligned} \tag{C.3}$$

where we use the harmonic polylogarithm function [67]

$$H_{011}(1-x) = \frac{1}{2} \log(1-x) \log^2 x + \log x \text{Li}_2(x) - \text{Li}_3(x) + \zeta_3. \tag{C.4}$$

Finally, the pentagon-box integral $I_5^{(2)b}$ has the small m^2 expansion

$$\begin{aligned}
s_2 s_3 s_5 I^{(2)b} = & -\frac{3}{4} \log^4 m^2 + \left[\log(s_1 s_2 s_3 s_4) - \frac{1}{3} \log(s_2 s_3 s_5) \right] \log^3 m^2 \\
& + \left[-\frac{3}{2} \log^2 s_1 - 2 \log s_2 \log s_1 - \log s_3 \log s_1 + 2 \log s_4 \log s_1 \right. \\
& + \log s_5 \log s_1 + \frac{3}{2} \log^2 s_2 + \log^2 s_3 - \log^2 s_4 + \frac{3}{2} \log^2 s_5 \\
& + \log s_2 \log s_3 - 2 \log s_2 \log s_4 - 2 \log s_3 \log s_4 \\
& - 2 \log s_2 \log s_5 - 2 \log s_3 \log s_5 + \log s_4 \log s_5 \\
& \left. - \text{Li}_2\left(1 - \frac{s_1}{s_3}\right) + \text{Li}_2\left(1 - \frac{s_2}{s_4}\right) - 2 \text{Li}_2\left(1 - \frac{s_2}{s_5}\right) - 2 \text{Li}_2\left(1 - \frac{s_3}{s_5}\right) + \frac{5\pi^2}{6} \right] \log^2 m^2 \\
& + \left[-2 H_{011}\left(1 - \frac{s_3}{s_1}\right) + 8 H_{011}\left(1 - \frac{s_4}{s_1}\right) - 6 H_{011}\left(1 - \frac{s_4}{s_2}\right) - 4 H_{011}\left(1 - \frac{s_3}{s_5}\right) \right. \\
& - 8 H_{011}\left(1 - \frac{s_5}{s_2}\right) - 4 \text{Li}_3\left(1 - \frac{s_3}{s_1}\right) + 4 \text{Li}_3\left(1 - \frac{s_4}{s_2}\right) - 4 \text{Li}_3\left(1 - \frac{s_3}{s_5}\right) \\
& + 4 \text{Li}_3\left(1 - \frac{s_5}{s_2}\right) + 2 \log\left(\frac{s_1 s_2 s_3}{s_4 s_5}\right) \text{Li}_2\left(1 - \frac{s_1}{s_3}\right) + 4 \log\left(\frac{s_1}{s_4}\right) \text{Li}_2\left(1 - \frac{s_1}{s_4}\right) \\
& + 2 \log\left(\frac{s_1 s_4 s_5}{s_2^3 s_3}\right) \text{Li}_2\left(1 - \frac{s_2}{s_4}\right) - 4 \log\left(\frac{s_2^2}{s_4 s_5^2}\right) \text{Li}_2\left(1 - \frac{s_2}{s_5}\right) \\
& + 4 \log\left(\frac{s_1 s_5}{s_3}\right) \text{Li}_2\left(1 - \frac{s_3}{s_5}\right) + \frac{8}{3} \log^3 s_1 + 2 \log s_2 \log^2 s_1 - 6 \log s_4 \log^2 s_1 \\
& - \log s_5 \log^2 s_1 + \log^2 s_2 \log s_1 + 5 \log^2 s_4 \log s_1 - \log^2 s_5 \log s_1 \\
& - 2 \log s_2 \log s_4 \log s_1 + 2 \log s_3 \log s_5 \log s_1 - \frac{1}{3} \pi^2 \log s_1 - \frac{17}{3} \log^3 s_2 \\
& - \log^3 s_3 + 3 \log^3 s_5 - \log s_2 \log^2 s_3 - 4 \log s_2 \log^2 s_4 + \log s_3 \log^2 s_4 \\
& \left. - 8 \log s_2 \log^2 s_5 - 2 \log s_3 \log^2 s_5 - \log s_4 \log^2 s_5 - \frac{2}{3} \pi^2 \log s_2 \right] \log m^2
\end{aligned}$$

$$\begin{aligned}
& -2 \log^2 s_2 \log s_3 - \frac{2}{3} \pi^2 \log s_3 + 6 \log^2 s_2 \log s_4 + 2 \log s_2 \log s_3 \log s_4 \\
& - \frac{1}{3} \pi^2 \log s_4 + 9 \log^2 s_2 \log s_5 + 2 \log^2 s_3 \log s_5 + 2 \log s_2 \log s_3 \log s_5 \\
& + \frac{1}{3} \pi^2 \log s_5 + 12 \zeta_3 \Big] \log m^2 + \mathcal{O}(\log^0 m^2)
\end{aligned} \tag{C.5}$$

When we sum over cyclic permutations to obtain the full one- and two-loop amplitudes, the polylogarithm functions cancel, resulting in the relatively simple expressions (3.3) and (3.8).

References

- [1] J.M. Drummond, J. Henn, V.A. Smirnov and E. Sokatchev, *Magic identities for conformal four-point integrals*, *JHEP* **01** (2007) 064 [[hep-th/0607160](#)] [[SPIRES](#)].
- [2] Z. Bern, L.J. Dixon, D.C. Dunbar and D.A. Kosower, *One-loop n-point gauge theory amplitudes, unitarity and collinear limits*, *Nucl. Phys. B* **425** (1994) 217 [[hep-ph/9403226](#)] [[SPIRES](#)].
- [3] Z. Bern, L.J. Dixon, D.C. Dunbar and D.A. Kosower, *Fusing gauge theory tree amplitudes into loop amplitudes*, *Nucl. Phys. B* **435** (1995) 59 [[hep-ph/9409265](#)] [[SPIRES](#)].
- [4] E.I. Buchbinder and F. Cachazo, *Two-loop amplitudes of gluons and octa-cuts in N = 4 super Yang-Mills*, *JHEP* **11** (2005) 036 [[hep-th/0506126](#)] [[SPIRES](#)].
- [5] Z. Bern, J.J.M. Carrasco, H. Johansson and D.A. Kosower, *Maximally supersymmetric planar Yang-Mills amplitudes at five loops*, *Phys. Rev. D* **76** (2007) 125020 [[arXiv:0705.1864](#)] [[SPIRES](#)].
- [6] F. Cachazo and D. Skinner, *On the structure of scattering amplitudes in N = 4 super Yang-Mills and N = 8 supergravity*, [arXiv:0801.4574](#) [[SPIRES](#)].
- [7] L.F. Alday and J.M. Maldacena, *Gluon scattering amplitudes at strong coupling*, *JHEP* **06** (2007) 064 [[arXiv:0705.0303](#)] [[SPIRES](#)].
- [8] J.M. Drummond, G.P. Korchemsky and E. Sokatchev, *Conformal properties of four-gluon planar amplitudes and Wilson loops*, *Nucl. Phys. B* **795** (2008) 385 [[arXiv:0707.0243](#)] [[SPIRES](#)].
- [9] A. Brandhuber, P. Heslop and G. Travaglini, *MHV amplitudes in N = 4 super Yang-Mills and Wilson loops*, *Nucl. Phys. B* **794** (2008) 231 [[arXiv:0707.1153](#)] [[SPIRES](#)].
- [10] J.M. Drummond, J. Henn, G.P. Korchemsky and E. Sokatchev, *On planar gluon amplitudes/Wilson loops duality*, *Nucl. Phys. B* **795** (2008) 52 [[arXiv:0709.2368](#)] [[SPIRES](#)].
- [11] J.M. Drummond, J. Henn, G.P. Korchemsky and E. Sokatchev, *Conformal Ward identities for Wilson loops and a test of the duality with gluon amplitudes*, *Nucl. Phys. B* **826** (2010) 337 [[arXiv:0712.1223](#)] [[SPIRES](#)].
- [12] Z. Bern, L.J. Dixon and V.A. Smirnov, *Iteration of planar amplitudes in maximally supersymmetric Yang-Mills theory at three loops and beyond*, *Phys. Rev. D* **72** (2005) 085001 [[hep-th/0505205](#)] [[SPIRES](#)].
- [13] L.F. Alday and J. Maldacena, *Comments on gluon scattering amplitudes via AdS/CFT*, *JHEP* **11** (2007) 068 [[arXiv:0710.1060](#)] [[SPIRES](#)].

- [14] J. Bartels, L.N. Lipatov and A. Sabio Vera, *BFKL Pomeron, Reggeized gluons and Bern-Dixon-Smirnov amplitudes*, *Phys. Rev. D* **80** (2009) 045002 [[arXiv:0802.2065](#)] [[SPIRES](#)].
- [15] Z. Bern et al., *The two-loop six-gluon MHV amplitude in maximally supersymmetric Yang-Mills theory*, *Phys. Rev. D* **78** (2008) 045007 [[arXiv:0803.1465](#)] [[SPIRES](#)].
- [16] J.M. Drummond, J. Henn, G.P. Korchemsky and E. Sokatchev, *Hexagon Wilson loop = six-gluon MHV amplitude*, *Nucl. Phys. B* **815** (2009) 142 [[arXiv:0803.1466](#)] [[SPIRES](#)].
- [17] L.F. Alday and R. Roiban, *Scattering amplitudes, Wilson loops and the string/gauge theory correspondence*, *Phys. Rept.* **468** (2008) 153 [[arXiv:0807.1889](#)] [[SPIRES](#)].
- [18] J.M. Henn, *Duality between Wilson loops and gluon amplitudes*, *Fortsch. Phys.* **57** (2009) 729 [[arXiv:0903.0522](#)] [[SPIRES](#)].
- [19] V. Del Duca, C. Duhr and V.A. Smirnov, *An analytic result for the two-loop hexagon Wilson loop in $N = 4$ SYM*, *JHEP* **03** (2010) 099 [[arXiv:0911.5332](#)] [[SPIRES](#)].
- [20] V. Del Duca, C. Duhr and V.A. Smirnov, *The two-loop hexagon Wilson loop in $N = 4$ SYM*, *JHEP* **05** (2010) 084 [[arXiv:1003.1702](#)] [[SPIRES](#)].
- [21] J.-H. Zhang, *On the two-loop hexagon Wilson loop remainder function in $N = 4$ SYM*, [arXiv:1004.1606](#) [[SPIRES](#)].
- [22] N. Beisert, J. Henn, T. McLoughlin and J. Plefka, *One-loop superconformal and Yangian symmetries of scattering amplitudes in $N = 4$ super Yang-Mills*, *JHEP* **04** (2010) 085 [[arXiv:1002.1733](#)] [[SPIRES](#)].
- [23] L.F. Alday, J.M. Henn, J. Plefka and T. Schuster, *Scattering into the fifth dimension of $N = 4$ super Yang-Mills*, *JHEP* **01** (2010) 077 [[arXiv:0908.0684](#)] [[SPIRES](#)].
- [24] G.P. Korchemsky, *Double logarithmic asymptotics in QCD*, *Phys. Lett. B* **217** (1989) 330 [[SPIRES](#)].
- [25] H. Kawai and T. Suyama, *Some implications of perturbative approach to AdS/CFT correspondence*, *Nucl. Phys. B* **794** (2008) 1 [[arXiv:0708.2463](#)] [[SPIRES](#)].
- [26] R.M. Schabinger, *Scattering on the moduli space of $N = 4$ super Yang-Mills*, [arXiv:0801.1542](#) [[SPIRES](#)].
- [27] J. McGreevy and A. Sever, *Planar scattering amplitudes from Wilson loops*, *JHEP* **08** (2008) 078 [[arXiv:0806.0668](#)] [[SPIRES](#)].
- [28] A. Gorsky and A. Zhiboedov, *Aspects of the $N = 4$ SYM amplitude – Wilson polygon duality*, *Nucl. Phys. B* **835** (2010) 343 [[arXiv:0911.3626](#)] [[SPIRES](#)].
- [29] R.H. Boels, *No triangles on the moduli space of maximally supersymmetric gauge theory*, *JHEP* **05** (2010) 046 [[arXiv:1003.2989](#)] [[SPIRES](#)].
- [30] J.M. Henn, S.G. Naculich, H.J. Schnitzer and M. Spradlin, *Higgs-regularized three-loop four-gluon amplitude in $N = 4$ SYM: exponentiation and Regge limits*, *JHEP* **04** (2010) 038 [[arXiv:1001.1358](#)] [[SPIRES](#)].
- [31] I.A. Korchemskaya and G.P. Korchemsky, *On lightlike Wilson loops*, *Phys. Lett. B* **287** (1992) 169 [[SPIRES](#)].
- [32] Z. Bern, M. Czakon, L.J. Dixon, D.A. Kosower and V.A. Smirnov, *The four-loop planar amplitude and cusp anomalous dimension in maximally supersymmetric Yang-Mills theory*, *Phys. Rev. D* **75** (2007) 085010 [[hep-th/0610248](#)] [[SPIRES](#)].

- [33] F. Cachazo, M. Spradlin and A. Volovich, *Four-loop cusp anomalous dimension from obstructions*, *Phys. Rev. D* **75** (2007) 105011, [[hep-th/0612309](#)] [[SPIRES](#)].
- [34] V.S. Fadin, R. Fiore and M.I. Kotsky, *Gluon regge trajectory in the two-loop approximation*, *Phys. Lett. B* **387** (1996) 593 [[hep-ph/9605357](#)] [[SPIRES](#)].
- [35] I.A. Korchemskaya and G.P. Korchemsky, *Evolution equation for gluon Regge trajectory*, *Phys. Lett. B* **387** (1996) 346 [[hep-ph/9607229](#)] [[SPIRES](#)].
- [36] A.V. Kotikov and L.N. Lipatov, *NLO corrections to the BFKL equation in QCD and in supersymmetric gauge theories*, *Nucl. Phys. B* **582** (2000) 19 [[hep-ph/0004008](#)] [[SPIRES](#)].
- [37] S.G. Naculich and H.J. Schnitzer, *Regge behavior of gluon scattering amplitudes in $N = 4$ SYM theory*, *Nucl. Phys. B* **794** (2008) 189 [[arXiv:0708.3069](#)] [[SPIRES](#)].
- [38] V. Del Duca and E.W.N. Glover, *Testing high-energy factorization beyond the next-to-leading-logarithmic accuracy*, *JHEP* **05** (2008) 056 [[arXiv:0802.4445](#)] [[SPIRES](#)].
- [39] S.G. Naculich and H.J. Schnitzer, *IR divergences and Regge limits of subleading-color contributions to the four-gluon amplitude in $N = 4$ SYM Theory*, *JHEP* **10** (2009) 048 [[arXiv:0907.1895](#)] [[SPIRES](#)].
- [40] R.C. Brower, H. Nastase, H.J. Schnitzer and C.-I. Tan, *Implications of multi-Regge limits for the Bern-Dixon-Smirnov conjecture*, *Nucl. Phys. B* **814** (2009) 293 [[arXiv:0801.3891](#)] [[SPIRES](#)].
- [41] R.C. Brower, H. Nastase, H.J. Schnitzer and C.-I. Tan, *Analyticity for multi-Regge limits of the Bern-Dixon-Smirnov amplitudes*, *Nucl. Phys. B* **822** (2009) 301 [[arXiv:0809.1632](#)] [[SPIRES](#)].
- [42] S. Catani, *The singular behaviour of QCD amplitudes at two-loop order*, *Phys. Lett. B* **427** (1998) 161 [[hep-ph/9802439](#)] [[SPIRES](#)].
- [43] G. Sterman and M.E. Tejeda-Yeomans, *Multi-loop amplitudes and resummation*, *Phys. Lett. B* **552** (2003) 48 [[hep-ph/0210130](#)] [[SPIRES](#)].
- [44] H.R.P. Ferguson and D.H. Bailey, *A polynomial time, numerically stable integer relation algorithm* <http://crd.lbl.gov/~dhbailey/dhbpapers/pslq.pdf>
- [45] P. Bertok, *PSLQ integer relation algorithm implementation*, <http://library.wolfram.com/infocenter/MathSource/4263/>.
- [46] V. A. Smirnov, *Feynman integral calculus*, Springer, Berlin Germany (2006).
- [47] M. Czakon, *MBasymptotics*, <http://projects.hepforge.org/mbtools/>.
- [48] M. Czakon, *Automatized analytic continuation of Mellin-Barnes integrals*, *Comput. Phys. Commun.* **175** (2006) 559 [[hep-ph/0511200](#)] [[SPIRES](#)].
- [49] N. Beisert, B. Eden and M. Staudacher, *Transcendentality and crossing*, *J. Stat. Mech.* (2007) P01021 [[hep-th/0610251](#)] [[SPIRES](#)].
- [50] D. Nguyen, M. Spradlin and A. Volovich, *New dual conformally invariant off-shell integrals*, *Phys. Rev. D* **77** (2008) 025018 [[arXiv:0709.4665](#)] [[SPIRES](#)].
- [51] R.J. Eden, P.V. Landshoff, D.I. Olive and J.C. Polkinghorne, *The analytic S-Matrix*, Cambridge University Press, Cambridge U.K. (1966).
- [52] P.D.B. Collins, *An introduction to regge theory and high-energy physics*, Cambridge University Press, Cambridge U.K. (1977).

- [53] I.G. Halliday, *High-energy behaviour in perturbation theory*, *Nuovo Cim.* **30** (1963) 177 [[SPIRES](#)].
- [54] G. Tiktopoulos, *High-energy behavior of Feynman amplitudes*, *Phys. Rev.* **131** (1963) 480 [[SPIRES](#)].
- [55] F. Cachazo, M. Spradlin and A. Volovich, *Iterative structure within the five-particle two-loop amplitude*, *Phys. Rev. D* **74** (2006) 045020 [[hep-th/0602228](#)] [[SPIRES](#)].
- [56] Z. Bern, M. Czakon, D.A. Kosower, R. Roiban and V.A. Smirnov, *Two-loop iteration of five-point $N = 4$ super-Yang-Mills amplitudes*, *Phys. Rev. Lett.* **97** (2006) 181601 [[hep-th/0604074](#)] [[SPIRES](#)].
- [57] V. Del Duca, C. Duhr and E.W. Nigel Glover, *The five-gluon amplitude in the high-energy limit*, *JHEP* **12** (2009) 023 [[arXiv:0905.0100](#)] [[SPIRES](#)].
- [58] A. Hodges, *The box integrals in momentum-twistor geometry*, [arXiv:1004.3323](#) [[SPIRES](#)].
- [59] L. Mason and D. Skinner, *Amplitudes at weak coupling as polytopes in AdS_5* , [arXiv:1004.3498](#) [[SPIRES](#)].
- [60] C. Anastasiou, Z. Bern, L.J. Dixon and D.A. Kosower, *Planar amplitudes in maximally supersymmetric Yang-Mills theory*, *Phys. Rev. Lett.* **91** (2003) 251602 [[hep-th/0309040](#)] [[SPIRES](#)].
- [61] A. Mitov and S. Moch, *The singular behavior of massive QCD amplitudes*, *JHEP* **05** (2007) 001 [[hep-ph/0612149](#)] [[SPIRES](#)].
- [62] C. Anastasiou et al., *Two-loop polygon Wilson loops in $N = 4$ SYM*, *JHEP* **05** (2009) 115 [[arXiv:0902.2245](#)] [[SPIRES](#)].
- [63] J.M. Drummond, J. Henn, G.P. Korchemsky and E. Sokatchev, *The hexagon Wilson loop and the BDS ansatz for the six-gluon amplitude*, *Phys. Lett. B* **662** (2008) 456 [[arXiv:0712.4138](#)] [[SPIRES](#)].
- [64] J. Bartels, L.N. Lipatov and A. Sabio Vera, *$N=4$ supersymmetric Yang-Mills scattering amplitudes at high energies: the Regge cut contribution*, *Eur. Phys. J. C* **65** (2010) 587 [[arXiv:0807.0894](#)] [[SPIRES](#)].
- [65] V. Gribov, *The theory of complex angular momenta*, Cambridge University Press, Cambridge U.K. (2003).
- [66] P.G. Federbush and M.T. Grisaru, *The high energy behavior of scattering amplitudes in perturbation theory*, *Ann. Phys.* **22** (1963) 263.
- [67] E. Remiddi and J.A.M. Vermaseren, *Harmonic polylogarithms*, *Int. J. Mod. Phys. A* **15** (2000) 725 [[hep-ph/9905237](#)] [[SPIRES](#)].